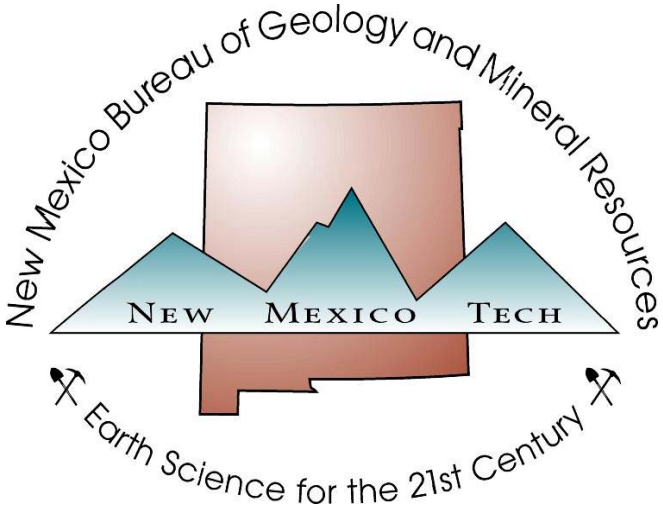

Initial paleoseismic and hydrologic assessment of the Southern Sangre de Cristo Fault at the Taos Pueblo site, Taos New Mexico

By

Keith I. Kelson, Paul W. Bauer, David Love, Sean D. Connell, Mark Mansell, and Geoffrey Rawling

Open-file Report 476

January 2004

WILLIAM LETTIS & ASSOCIATES, INC.

Technical Report

Initial Paleoseismic and Hydrologic Assessment of the Southern Sangre de Cristo Fault at the Taos Pueblo Site

Taos, New Mexico

Prepared for:

New Mexico Bureau of Geology and Mineral Resources
State of New Mexico Department of Public Safety
Pueblo of Taos

Prepared by:

William Lettis & Associates, Inc.
1777 Botelho Drive, Suite 262
Walnut Creek, CA 94596

New Mexico Bureau of Geology and Mineral Resources
801 Leroy Place
Socorro, NM 97801

WLA

TECHNICAL REPORT

INITIAL PALEOSEISMIC AND HYDROGEOLOGIC ASSESSMENT OF THE SOUTHERN SANGRE DE CRISTO FAULT AT THE TAOS PUEBLO SITE, TAOS COUNTY, NEW MEXICO

Prepared for:

New Mexico Bureau of Geology and Mineral Resources
State of New Mexico Department of Public Safety
Pueblo of Taos

Prepared by:

Keith I. Kelson[1], Paul W. Bauer[2], David Love[2], Sean D. Connell[2], Mark Mansell[2], and Geoffrey Rawling[2]

[1]William Lettis & Associates, Inc.
1777 Botelho Drive, Suite 262
Walnut Creek, CA 94596
kelson@lettis.com

[2]New Mexico Bureau of Geology and Mineral Resources,
801 Leroy Place
Socorro, NM 87801
bauer@gis.nmt.edu, dave@gis.nmt.edu, connell@gis.nmt.edu, grawling@gis.nmt.edu

January 2004

WILLIAM LETTIS & ASSOCIATES, INC.
1777 Botelho Drive, Suite 262, Walnut Creek, California 94596
tel (925) 256-6070 fax (925) 256-6076

January 20, 2004

Dr. Paul Bauer
New Mexico Bureau of Geology and Mineral Resources
801 Leroy Place
Socorro, NM 87801

Subject: Initial Paleoseismic and Hydrogeologic Assessment of the Southern Sangre de Cristo Fault at the Taos Pueblo Site, Taos County, New Mexico

Dear Paul:

Enclosed please find nine bound copies and one unbound copy of our technical memorandum summarizing our recent trenching effort on the Taos Pueblo. Also enclosed is a compact disc containing the entire memo (including figures and tables) as a PDF file. As you know, the focus of this work was on the southern Sangre de Cristo fault, which runs through Taos Pueblo near the base of the Sangre de Cristo Mountains. The main goal of this work is to document the characteristics of the fault in the shallow subsurface. This effort provides information on the timing of the most-recent large earthquake on the fault, and on how the fault influences shallow groundwater flow.

The Sangre de Cristo fault is recognized as a potential source of large earthquakes, and as an important control on groundwater flow in the shallow subsurface. Understanding the earthquake history of the Sangre de Cristo fault helps characterize the likelihood of future large earthquakes in northern New Mexico. Also, understanding the near-surface characteristics of the fault is helpful for modeling the directions and rates of shallow groundwater flow.

The Taos Pueblo site was chosen for this investigation because it is one of only a few sites where the main strand of the southern Sangre de Cristo fault is clearly developed in alluvial-fan deposits west of the Sangre de Cristo Mountains. Our detailed topographic surveying at the trench site suggests two large earthquakes have occurred on the fault in geologically recent times. Each of these surface ruptures probably produced about 1.5 m (about 5 ft) of vertical uplift, which suggests the occurrence of large earthquakes having magnitudes in the range of **M**6.5 to **M**7.5. Geologic relations exposed in this study suggest that the most-recent large earthquakeon the southern Sangre de Cristo fault occurred about 10,000 to 30,000 years ago. In addition, the fault characteristics developed in this study suggest that shallow groundwater percolating downward from the ground surface probably flows westerly until it encounters the fault, and then percolates downward along the fault. These relations suggest that major fault strands of the southern Sangre de Cristo fault act as preferential pathways for downward groundwater flow in the unconsolidated, near-surface materials.

This trenching effort was completed by Keith Kelson of WLA, and Paul Bauer, Dave Love, Sean Connell, Geoffrey Rawling, and Mark Mansell of the New Mexico Bureau of Geology and Mineral Resources. Please feel free to contact me if there are any questions or if we can be of further assistance.

Respectfully,

Keith I. Kelson
Principal Geologist

enclosures (10 reports, 1 CD)

INITIAL PALEOSEISMIC AND HYDROGEOLOGIC ASSESSMENT OF THE SOUTHERN SANGRE DE CRISTO FAULT AT THE TAOS PUEBLO SITE, TAOS COUNTY, NEW MEXICO

ABSTRACT

The primary goals of this investigation are to provide information on (1) large, geologically recent earthquakes along the southern Sangre de Cristo fault, and (2) document fault characteristics in the shallow subsurface to help evaluate influences of the fault on vadose zone groundwater flow. The 240-km-long Sangre de Cristo fault shows prominent geomorphic evidence of geologically recent surface rupture, and is recognized as a significant potential source of large earthquakes. The data obtained from this effort will be applicable to other similar faults throughout northern and central New Mexico. Defining the earthquake history of the Sangre de Cristo fault helps reduce the uncertainty in characterizing earthquake sources throughout the Rio Grande rift, including possible fault ruptures close to Santa Fe, Albuquerque, and other areas in New Mexico. Also, this work documents the near-surface characteristics of faults in alluvial materials, to help constrain vadose-zone groundwater modeling.

The Taos Pueblo site was chosen for this investigation because it has (1) excellent geomorphic relations that constrain the location of the main strand of the fault, (2) late Pleistocene alluvial-fan deposits on the mountain-front piedmont, and (3) minimal cultural disturbance. Our detailed topographic surveying of the site vicinity shows that the primary fault scarp crosses late Pleistocene alluvial-fan deposits and exhibits about 3 m of net vertical tectonic displacement. A distinct bevel in the scarp profile at the trench site suggests the occurrence of two surface ruptures since deposition of the alluvial fan, each with about 1.5 m of vertical displacement. These displacements are consistent with large earthquakes having magnitudes in the range of **M**6.5 to **M**7.5.

This investigation involved a characterization of the fault based on a trench excavation across a prominent fault scarp, detailed topographic surveying, and analysis of two soil test pits adjacent to the trench. Stratigraphic relations exposed in the trench show the presence of middle Pleistocene eolian and alluvial-fan deposits on the western, upthrown side of the fault, and probable late Pleistocene alluvial and colluvial deposits on the eastern, downthrown side of the fault. Stratigraphic evidence of surface-fault rupture is restricted to a package of scarp-derived colluvium on the downthrown side of the fault. This colluvial package includes fissure-fill and near-scarp deposits that probably were deposited immediately following the surface rupture. The moderately developed soil formed on this colluvial package is interpreted to be approximately 10,000 to 30,000 years old. Thus, the trench exposure suggests that the

most-recent surface rupture along the southern Sangre de Cristo fault occurred about 10,000 to 30,000 years ago.

The main fault strand at the trench site is located near the base of the topographic scarp, and consists of a primary west-dipping fault plane and secondary faulting within a 6-m-wide zone on the hanging wall. The primary fault zone contains multiple anastomosing strands within the sheared alluvium, with strands commonly bordering lentil-shaped bodies of sediments. The pervasive shearing within the fault zone probably represents a zone of lower permeability compared to surficial deposits east of the fault, but a zone of higher permeability compared to deposits west of the fault. The bulk permeability likely is anisotropic with greater permeability down the fault zone rather than across it. Several near-vertical fractures within the fault zone are associated with calcium carbonate accumulations, suggesting that downward percolation of meteoric water occurs preferentially along these fractures. The trench shows the presence of calcium carbonate cementation commonly along fault planes in fine- and medium-grained deposits, as well as intersecting patterns of subhorizontal and subvertical accumulations that likely are related to vadose-zone groundwater processes. The cementation locally observed along the fault exposed in the trench may be indicative of preferential groundwater flow downdip along the fault. Thus, the relations exposed in the trench suggest that major fault strands of the southern Sangre de Cristo fault act as preferential pathways for downward vadose-zone groundwater flow in unconsolidated near-surface materials.

TABLE OF CONTENTS

1.0 INTRODUCTION

1.1 Project Goals

The primary goals of this investigation are to provide information on (1) large, geologically recent earthquakes along the southern Sangre de Cristo fault, and (2) document fault characteristics in the shallow subsurface to help evaluate influences of the fault on vadose zone groundwater flow. This investigation involved a characterization of the fault based primarily on documenting a trench excavation across a prominent fault scarp produced by pre-historic surface rupture. The study also included collection of detailed topographic data at the Taos Pueblo trench site, and analysis of two soil test pits adjacent to the trench. This effort is the first-ever trench evaluation of the southern Sangre de Cristo fault in northern New Mexico. This study provides preliminary information on the late Pleistocene to Holocene history of large, surface-rupture earthquakes along the fault, as well as a documentation of shallow fault characteristics where it displaces unconsolidated surficial deposits.

1.2 Project Significance

Obtaining information on the timing and size of prehistoric surface fault ruptures on the southern Sangre de Cristo fault is important for estimating the probability and magnitude of future earthquakes on the fault. The southern Sangre de Cristo fault is the most prominent rift-margin normal fault in the Rio Grande rift of northern New Mexico, and arguably is the most likely source of large earthquakes in northern New Mexico (Wong et al., 1996; Kelson and Olig, 1995; Machette et al., 1998). The fault exhibits geomorphic evidence for several large earthquakes in the past few hundred thousand years (Machette and Personius, 1984; Menges, 1988, 1990). However, there are no detailed data on the timing of large, surface-rupturing earthquakes along the fault. Such data are critical for reliably forecasting the potential for future large earthquakes, and the overall seismic hazard, in northern New Mexico.

Because the Sangre de Cristo fault is one of the largest faults in the northern Rio Grande rift, data obtained through this work is applicable to other similar, poorly characterized faults throughout northern New Mexico. In particular, major rift faults within the Albuquerque-Santa Fe corridor of central New Mexico either are located in highly eroded terrain, buried by latest Holocene alluvium, poorly expressed, or are inaccessible for geologic research. The southern Sangre de Cristo fault is comparatively well expressed, and thus provides an excellent opportunity for characterizing major rift faults. Thus, defining the long-term earthquake history of the Sangre de Cristo fault helps reduce the uncertainty in characterizing earthquake sources throughout the Rio Grande rift, including possible fault ruptures close to Santa Fe, Albuquerque, and other areas in New Mexico. Also, this work documents the near-surface characteristics of the fault in unconsolidated materials, to help constrain groundwater modeling efforts.

2.0 GEOLOGIC SETTING OF THE TAOS PUEBLO SITE

On the basis of detailed geologic mapping of the Taos area (Bauer et al., 2001), the Taos Pueblo site provides one of the best opportunities to assess the earthquake history on the southern Sangre de Cristo fault, and to assess the near-surface characteristics of the fault where it deforms young deposits within the groundwater vadose zone. This southern Sangre de Cristo fault forms the eastern border of the actively subsiding San Luis rift basin, and has had west-down displacement over recent geologic time. The fault is divided into four sections and numerous subsections on the basis of fault-trace complexity and mountain-front and fault-scarp morphologic data (Menges, 1988; Machette et al., 1998). This study focused on a site along the 14-km-long southern section of the fault (e.g., the "Cañon section" of Machette et al., 1998). This site is on land under the jurisdiction of Taos Pueblo, about 2 km northeast of the Town of Taos plaza (Figure 1).

The southern Sangre de Cristo fault shows prominent geomorphic evidence of geologically recent surface rupture, including scarps across alluvial fans of various ages, air-photo lineaments, springs, and alignments of vegetation. Machette and Personius (1984) and Personius and Machette (1984) profiled several scarps along the Cañon section, and suggest a Holocene age (within the past 11,000 years) for the most-recent movement. Kelson (1986) mapped late Quaternary deposits and some fault strands along this section, and showed faulted late Pleistocene alluvial-fan deposits. Menges (1990) conducted detailed morphometric analyses of the range front and fault scarps, and suggested the possibility of early Holocene to latest Pleistocene movement along the Cañon section. Recent detailed geologic mapping along the fault (Bauer et al., 2001) supports these estimates. Based on scarp morphology data, Menges (1988, 1990) estimated a recurrence interval of about 10,000 to 50,000 years between large earthquake ruptures. However, there have been no paleoseismic trench investigations of the southern Sangre de Cristo fault, and the exact timing of past surface ruptures on the southern Sangre de Cristo fault is unknown.

The Taos Pueblo site was chosen for this investigation because it has: (1) excellent geomorphic relations that constrain the location of the main strand of the fault; (2) late Pleistocene alluvial-fan deposits on the mountain-front piedmont; and (3) minimal cultural disturbance. The site is on the moderately west-sloping piedmont along the Sangre de Cristo mountain front, which contains a coalescent alluvial-fan complex derived from large and small drainages in the range (Figure 2). The alluvial fans consist primarily of coarse deposits derived from Pennsylvanian-age bedrock in the Sangre de Cristo Mountains, which include primarily sandstone and siltstone with local limestone interbeds (Bauer et al., 2001).

The Sangre de Cristo fault zone likely consists of at least three fault strands in the site vicinity (Figure 2), including strands associated with: (1) the break-in-slope at the base of the bedrock range front east of the site; (2) a prominent west-facing scarp on the piedmont at the trench site, and (3) a subtle, broad west-facing scarp on the piedmont about 0.6 km west of the trench site. We believe that the prominent strand traversing our trench site is the primary late Quaternary fault strand, although testing this interpretation is beyond the scope of this investigation. Directly south of the trench site, this central fault strand splits into two strands and also is associated with a subtle splay fault east of the trench site (Figure 2). Trench T-1 is located across the most prominent strand of the Sangre de Cristo fault at this latitude.

The prominent fault scarp traversing the site is developed across a Pleistocene alluvial-fan complex (map unit Qfu, Figure 2). This map unit includes several individual alluvial-fan deposits and surfaces that are difficult to correlate on a regional scale, and thus our mapping groups these deposits as "undifferentiated Pleistocene alluvial-fan deposits" (Bauer et al., 2001). These deposits are distinguished from "young alluvial-fan deposits" (map unit Qfy, Figure 2), which are stratigraphically inset into map unit Qfu, have a lesser degree of soil-profile development, and generally are associated with present-day arroyos or areas of active alluviation. Bauer et al. (2001) estimated that map unit Qfy is Holocene to latest Pleistocene in age, and that map unit Qfu is middle to late Pleistocene in age. In the trench site vicinity, the prominent fault strand cuts across three different alluvial-fan surfaces, each of which is displaced a different amount. We surveyed the site vicinity using a differential global positioning system (DGPS) (Figure 3). This detailed topographic profiling shows that the primary scarp represents about 3 m of net vertical tectonic displacement (Figure 4). In addition, two secondary scarps also show displacement of the fan surface about 1 m each (Figure 4A). A profile completed in 1980 by M. Machette (personal communication, 2003; Machette and Personius, 1984) suggests a net surface displacement of 2.8 m across the primary fault scarp. Topographic profiling also shows that the alluvial fan surface directly north of the trench site is displaced a total of 7 ± 1 m (unpublished data, this study), and the fan surface about 400 m north of the site is displaced 9 ± 1m (Bauer et al., 2001). In addition, detailed topographic surveying of the trench site shows that the primary fault scarp is progressively higher from the trench site to the north (Figure 5). A derivative slope map generated from the topographic map shows that the steepest part of the scarp at the trench site has a small section that is between 9˚ and 13˚, whereas the scarp north of the trench site has a longer section of the scarp within this range in slope angle (Figure 6). We interpret these data to indicate the occurrence of multiple surface ruptures along this fault strand over the past several tens of thousands of years or more.

The morphology of the primary scarp at the Taos Pueblo site includes a distinct scarp bevel that may reflect the occurrence of multiple surface-rupturing earthquakes. As shown on Figure 3C, the steep, central part of the scarp is flanked by sections that are less steep. Projections of the gradients of these

bevels suggest that the central part of the scarp is associated with about 1.5 m of net vertical tectonic displacement (NVTD). Overall, the NVTD for the entire primary scarp is about 3 m (Figure 4C). These relations suggest the occurrence of two surface ruptures since the formation of the alluvial-fan surface, each with about 1.5 m of NVTD. On the basis of these data, we hypothesized prior to trenching that trenching across the primary fault scarp could provide evidence of two past surface ruptures since the deposition of the late Pleistocene alluvial fan. These displacements would be consistent with large earthquakes having magnitudes in the range of **M**6.5 to **M**7.5.

3.0 PALEOSEISMIC AND SOIL STRATIGRAPHIC RESULTS

Trench T-1 was excavated across the west-facing fault scarp developed on latest Pleistocene alluvial-fan deposits (Figure 7). We excavated soil test pit T-2 on the upthrown (eastern) side of the fault, and test pit T-3 on the downthrown side of the fault, to assess the characteristics of near-surface soils on both sides of the fault (Figure 5). These excavations exposed faulted alluvial deposits and scarp-derived colluvial deposits from which to evaluate the number and timing of surface ruptures and thus to characterize the earthquake history on the fault. The trenches were excavated using a standard rubber-tire backhoe and were shored for worker safety according to OSHA regulations (Figure 7). After cleaning the trench walls, stratigraphic and structural relations were flagged and surveyed using a Topcon GTS-303 total station. Print outs of these data were then used as a base map for manual logging of the exposures. We logged both walls of trench T-1 in detail near the fault, whereas test pits T-2 and T-3 were either sketch logged or described without logging. After documentation of the exposures, the trench and test pits were backfilled with the excavated material, and the site was restored to its original grade.

3.1 Trench Stratigraphy

Trench T-1 exposed a sequence of Pleistocene and Holocene alluvial, colluvial, and possibly eolian deposits (Figure 8). In general, deposits east of the fault scarp consist of primarily massive silty sand (of possible eolian and minor fluvial origin), which is overlain by coarse alluvial-fan deposits derived fron the Sangre de Cristo Mountains. For ease of description, we herein refer to the possible eolian deposits as unit 1, and the coarse alluvial-fan deposits collectively as unit 2 (Figure 8). On the western side of the fault, the deposits consist of coarse- and fine-grained alluvial deposits (units 3 and 4), which are overlain by carbonate-cemented alluvium or colluvium (units 5 and 6). These units are cross-cut by vertically oriented, well-mixed deposits (units 7 and 8) that may be fissure fills related to surface ruptures. Overlying these deposits is a package of scarp-derived colluvium, including a coarse proximal colluvium (unit 9) that grades upward into a finer-grained distal colluvium (unit 10). The uppermost deposit exposed in the trench is a coarse- to medium-grained gravelly and sandy colluvium that reflects active transport of material down the fault scarp (unit 11). The lithologic characteristics of these deposits are summarized in the following text, and are provided in more detail on Figures 8, 9, and 10. Soil characteristics exposed in the excavations are tabulated in Table 1. At the present time, there are no numerical or correlative age-estimates available for the stratigraphy exposed at the Taos Pueblo site. Our rough age estimates for the surficial deposits at the site, as given below, are based on the characteristics of soils developed in the deposits, stratigraphic position, and site geomorphology.

Unit 1 is the oldest deposit exposed in the trench (Figures 8, 9, and 10), consisting primarily of massive silt and clay that represents eolian deposition along the Sangre de Cristo mountain front. The uppermost

part of this deposit contains thin clayey sand beds, suggesting slight re-working of the deposit by small channels. On the basis of stratigraphic position, we interpret that unit 1 is middle Pleistocene in age. Unit 2 consists of coarse-grained gravel within several alluvial channels cut onto underlying eolian sands. Gravel clasts range in size up to 36 cm, have crude imbrication, and consist primarily of sandstone and siltstone lithologies. In exposure T-3, this older alluvium is the parent material for a well-developed cemented carbonate soil horizon; in trench T-1 the gravel is locally cemented and may represent a lower soil-stratigraphic horizon. Margins of gravel channels exposed in the trench T-1 wall suggest northwesterly to northerly flow directions. These deposits represent alluvial-fan deposits derived from the Sangre de Cristo Mountains. On the basis of well-developed soil characteristics and stratigraphic position, we interpret that unit 2 is middle Pleistocene in age.

Units 3 and 4 are alluvial deposits exposed only on the western (downthrown) side of the fault in trench T-1 (Figures 8, 9, and 10). Unit 3, which is the lowest stratigraphic unit exposed on the downthrown side of the fault, consists of sandy gravel with clasts up to 30 cm in diameter, grading upward into gravelly sand. Unit 3 grades upward into unit 4, which is a silty sand with few or no gravel clasts. Unit 4 contains an intersecting pattern of subhorizontal and subvertical calcium carbonate accumulations that likely are related to vadose-zone groundwater processes. Collectively, units 3 and 4 represent a fining-upward alluvial sequence, probably deposited as part of the coalescent alluvial-fan complex along the western margin of the Sangre de Cristo mountain front. The age of these deposits is speculated to be middle to late Pleistocene.

Units 5 and 6 also are exposed only on the western (downthrown) side of the fault in trench T-1 (Figures 8, 9, and 10), and consist of a second fining-upward alluvial sequence. Unit 5 contains sand and gravel, with a greater number of clasts (and larger clasts) adjacent to the main fault strand (Figure 9). In addition, unit 5 also contains slightly more clasts directly west of the secondary fault strand (Station 21m, Figures 9 and 10). Unit 5 grades upward into unit 6, which is a light pink-colored clayey sand with locally discontinuous stone lines. Unit 6 is strongly effervescent and pervasively cemented with calcium carbonate. Units 5 and 6 likely also represent deposition as part of the coalescent alluvial-fan complex along the Sangre de Cristo mountain front. The Sangre de Cristo fault clearly displaces both of these deposits, and well-developed fault planes are associated with rotated clasts and shear fabric within these units. The well-developed stage III+ soil suggests that these deposits are middle to late Pleistocene in age.

Unit 7 consists of two separate, near-vertical bodies along the primary and secondary strands of the Sangre de Cristo fault exposed in trench T-1 (Figures 8, 9, and 10). This unit is composed of sand and gravel similar in size and sorting to units 4, 5 and 6. Along the primary fault strand (Stations 25m to 26m;

Figures 8, 9, and 10), unit 7 is loose, pervasively sheared and most clasts have vertical orientations. This material likely is fault gouge produced through shearing and tectonic deformation of units 2 and 5. Along the secondary fault strand (Station 21m, Figures 8, 9, and 10), unit 7 is dense, finer-grained, and has less internal shearing. The origin of this material is uncertain, although it likely is fault gouge associated with deformation of units 4, 5 and 6 during movement along the secondary fault strand. Alternatively, the lesser amount of shearing in the body of unit 7 at Station 21m suggests that this material may be a fissure fill deposited into an open surface-rupture fracture.

We interpret that units 8, 9 and 10 were deposited locally along the scarp following the most-recent surface rupture. Unit 8 consists of several local, discontinuous deposits of sand and gravel along either primary or secondary fault strands. Gravel clasts within this unit commonly have sub-vertical orientations and are similar in size and rounding to those in adjacent deposits (i.e., units 2 or 6), which are the likely sources of material for unit 8. The cross-sectional shape of the separate deposits comprising unit 8 strongly suggests deposition within open fissures or depressions along the fault. Unit 8 grades upward into unit 9, which onlaps the lower and middle parts of the fault scarp (Figure 8). The base of unit 9 near the fault is sandy gravel, and the unit is finer upward and away from the fault. The size and rounding of the gravel clasts is consistent with derivation from the older alluvium forming the scarp crest (unit 2), and unit 9 clearly is coarser where it directly overlies this alluvium (Figures 9 and 10). The orientations of gravel clasts within unit 9 are parallel to the depositional slope, and also support an interpretation that this deposit is the proximal facies of a scarp-derived colluvium. Unit 9 grades upward into unit 10, which contains fewer gravel clasts and also represents deposition on the downthrown side of the fault. A moderately developed soil has formed on units 9 and 10, including a soil Btk horizon and stage I calcium carbonate accumulation within the colluvial sequence. These soil characteristics suggest a latest Pleistocene age, which we speculate to be on the order of about 10,000 to 30,000 years.

The uppermost surficial deposit exposed in Trench T-1 is unit 11, which unconformably overlies unit 2 east of the fault, and units 9 and 10 west of the fault (Figure 8). This uppermost unit consists of silty sand to clayey sand, with some gravel clasts. In particular, the gravel distribution within unit 11 directly reflects local underlying units, such that unit 11 contains abundant gravel where it overlies units 2 and 9 but contains fewer clasts where it overlies unit 10 (Figure 8). Overall, unit 11 represents the active hillslope colluvium across the remnant fault scarp, and is Holocene in age.

3.2 Soil-Stratigraphic Relations

3.2.1 Soil-Profile Development

Soil profiles were described in excavated trenches in order to aid in lithologic correlations across the fault and to estimate deposit ages. Field based soil-morphologic descriptions are generally reliable indicators of relative surface age and stability (e.g., McFadden et al., 1989) and have been used throughout the region to construct alluvial chronologies that can provide correlative age control for Quaternary landforms and associated deposits (e.g., Gile et al., 1981; Machette, 1985). Soil-profile morphology was described using a standard system of diagnostic criteria and nomenclature developed by the Soil Conservation Service (Soil Survey Staff, 1951, 1975, 1992 and 1993), and Gile et al. (1966), with modifications after Birkeland (1984). Soil properties recorded at each site include horizon designation, depth, thickness, dry and moist color, texture, structure, dry and moist consistence, clay film development, clast (stone) content, root and pore development, pedogenic carbonate development and morphology and lower horizon boundary characteristics (Birkeland, 1984). Carbonate-morphological stages were determined using nomenclature of Gile et al. (1966, as modified by Birkeland, 1984). The "+" symbol (e.g., stage III+) denote soils that exhibit a strongly developed morphologic stage. Colors are described using Munsell (1992) notation. The vertical arrangement of soil horizons and associated properties were described from the land surface down to the base of the excavation. Comparisons to inferred parent material were made to materials at the base of soil profiles and in nearby active stream channels.

A number of geomorphic and soil-based alluvial chronologies in the region provide correlative age constraints and are used to estimate ages of soil-bounded alluvial deposits exposed in the trench excavations. Some of these studies are in the southern San Luis basin (Kelson, 1986; Pazzaglia, 1989; Pazzaglia and Wells, 1990), western Jemez Mountains and adjacent Española basin (Dethier et al., 1988; Gonzalez, 1995; Reneau and McDonald, 1996; McDonald et al., 1996; Drakos and Reneau, 2003), eastern Colorado Plateau (Grimm, 1985; Drake et al., 1991), northern Albuquerque-Belen sub-basins (Machette, 1985; Connell and Wells, 1999), and southern New Mexico (Gile et al., 1981, 1995).

The development of soils depends on a variety of factors, such as parent material texture and composition, vegetation, climate, slope aspect, and age (Birkeland, 1984). Soils form when the rate of soil development exceeds the rate of sedimentation or erosion of the host deposit. Thus, the degree of soil development can be used to estimate durations of relative landscape stability. Soils of the study area contain horizons with pedogenic clay and carbonate. Pedogenic clays (argillans) have translocated (moved) down through the soil profile after stabilization of the deposit surface. Pedogenic clays commonly are recognized by the presence of clay films in root pores, in the interstices between sand grains, as colloidal stains on grains, or along ped faces. Soils containing pedogenic clay films are denoted by Bt

horizons. Pedogenic carbonate is recognized by the accumulation of micritic calcium carbonate in soil horizons are denoted as Bk horizons, which are typically paler in color than carbonate-free horizons. Soils in the study area trenches contain horizons that range from disseminated calcium carbonate to Stage I to III+ carbonate morphology. Some horizons exhibit both pedogenic clay and carbonate and are designated as Btk horizons. The presence of both pedogenic clay and carbonate within a soil horizon indicates that development under at least two distinct soil-moisture regimes. The calcium ion in carbonate cements flocculates clay and inhibits clay film development (Birkeland, 1984). The presence of argillans and carbonate indicates that soils probably existed through at least one change in climate, probably from moister to drier climatic conditions. The presence of Btk horizons suggest that such soils likely formed during moisture times when carbonate was effectively flushed out of the solum. During subsequent times of increased aridity, carbonate accumulated in the solum.

In general, soils that exhibit Stage I to II carbonate morphology are interpreted to be early Holocene to latest Pleistocene in age, and soils that exhibit Stage III and IV carbonate morphology are commonly interpreted to be late to middle Pleistocene in age (e.g., Machette, 1985; Kelson, 1986; Pazzaglia and Wells, 1996; McDonald et al., 1996). Soils having few and thin clay films are interpreted to be early Holocene or latest Pleistocene in age, whereas common, thick, and more strongly developed argillans are commonly found in older deposits.

Soils in the study area are complex, locally cumulic, polygenetic, and possess both translocated, micritic calcium carbonate and clay. Multiple soils are differentiated using an alphabetic code in order to avoid confusion with mapped lithologic units. There are at least five distinct soils (A-E) recognized in the trench excavations. A young veneer of sediment mantles much of the ground surface and is described below, but is not included as a distinct soil, but rather as a thin surficial deposit (see below). The youngest soil is designated as Soil A. Successively older soils are differentiated on the basis of stratigraphic superposition and are designated from youngest to oldest. Most soils are described along a vertical transect in the trenches; however, the soils of Pedon 1C were described over a horizontal distance of about 1.5 m in Trench T-1 (Figure 8) in order to better characterize soil variability on the hanging wall of the fault.

3.2.2 Surface Deposit

The study area is mantled by a <5 cm thick accumulation of reddish-brown wind-blown clay, sandy clay loam, and sandy loam that is recognized in all trench exposures. This thin veneer is recognized as the top of unit 11, but is too thin to differentiate in the trench exposures. This deposit is loose, exhibits minimal to no soil structure, and contains only sparse disseminated carbonate and abundant roots. The deposit is widespread and commonly obscures constructional bar-and-swale topography in underlying fluvial units.

This pedogenically unaltered deposit likely represents eolian deposition of dust downwind of the floor of the San Luis basin, about 4 km to the west. This thin, relatively unaltered soil C-horizon is not considered in discriminating surface soils from buried paleosols.

3.2.3 Soil A

Soil A is recognized in all trench exposures and developed in units 9, 10, and 11. This soil is a brown sandy clay loam to silty clay loam with moderate medium to coarse subangular blocky structure and few, thin colloidal stains on sand grains. Deposits contain disseminated carbonate and Stage I pedogenic carbonate morphology. Horizons containing both clay and carbonate (Btk) are 40 to 184 cm thick in the trenches and exhibit Stage I+ carbonate morphology, medium to strong angular blocky to prismatic soil structure and thin clay films, which are recognized as colloidal stains on grains and clay films on pore fillings and ped faces. The presence of both pedogenic clay and carbonate development in units 9, 10, and 11 indicates that this soil has been subjected to different soil-moisture regimes. Comparisons of soil-profile development to soil-based alluvial chronologies along the western front of the Sangre de Cristo Mountains, between Arroyo Seco and just north of Red River (Pazzaglia and Wells, 1990) and to the Jemez Mountains (Reneau and McDonald, 1996; Drakos and Reneau, 2003), support an early Holocene(?) or latest Pleistocene age (>5,000 and <~30,000 yrs) for units 9 and 10. Perhaps this soil began forming during a wetter period, such as during the latest Pleistocene. Pedogenic carbonate then migrated through the solum during drier conditions of the Holocene. This would indicate that the soil developed on units 9 and 10 began forming prior to Holocene time, or about 10,000 to 30,000 years ago.

3.2.4 Soil B

Soil B is developed in unit 6 and represents colluvial deposits that are likely associated with the penultimate surface rupture along the fault in the study area. This soil contains both pedogenic clay and exhibits State I+ carbonate morphology (Btk). The clay films are significantly thicker and more abundant than in the overlying soil. The abrupt, wavy to irregular upper contact suggests that this soil has been partially stripped. The stratigraphic position of this soil and comparisons of soil-profile development to soil-based alluvial chronologies in the region suggest that Soil B is at least 10,000 years old and probably formed during late Pleistocene time (>10,000 and <128,000 yrs ago).

3.2.5 Soil C

Soil C is developed in depositional units 3 and 4 exposed in Trench T-1. This soil has a moderately developed calcic Bk horizon with Stage III pedogenic carbonate morphology. This degree of soil development is similar to, but not correlative with, Soil D. Stratigraphic position and comparisons to soil-

based alluvial chronologies in the region indicate that this soil is much older than the Holocene and probably formed during the late or middle Pleistocene.

3.2.6 Soil D

Soil D is developed in unit 2, which is a white- to brown weakly to unconsolidated gravelly sand with a matrix that is dominantly loamy sand to sandy loam with weakly developed subangular blocky structure. In trench T-1, the upper 100 cm is dominated by pedogenic carbonate and exhibits Stage III+ pedogenic carbonate morphology. Pedogenic clay is also present and forms Btk horizons within the gravelly sand. In trench T-2, a lack of associated and overlying Bt horizons and a sharp erosional upper contact indicates that the top of this soil has been partially stripped. The presence of numerous subhorizontal and subvertical micritic carbonate stringers suggest that this unit has experienced groundwater cementation. The character of these carbonate cementation patterns are complicated and obscured by krotovina (animal burrows). Based on the stratigraphic position of this soil, degree of soil-profile development, and comparison to other soil-based alluvial chronologies in the region, this deposit is likely middle Pleistocene in age and probably formed between 130,000 to 250,000 years ago.

3.2.7 Soil E

The stratigraphic position of Soil E (unit 1) indicates that this the oldest unit exposed in the study area trenches. Unit 1 is a pinkish-white and yellowish-brown to strong brown, massive clay and silt with thin tabular to lenticular clayey sand beds. The deposit is moderately to well consolidated and possesses hard consistence and exhibits moderate to strong angular blocky to prismatic soil structure. Primary depositional fabric is intact, although there is little evidence for preservation of a complete soil at the top of this unit and the presence of a scoured upper contact indicates that the top of this unit has been partially stripped. The upper 87 cm contains pedogenic carbonate that forms Stage I and II carbonate morphology. The lower part of this unit contains carbonate only in root tubes, where it is commonly disseminated; the matrix is noncalcareous. The presence of both pedogenic clay and carbonate indicates that this soil formed during different surface moisture regimes. Because the top of this unit has been scoured, it is not possible to determine if the preserved soil represented the top of this unit, or a buried soil. Because this unit is buried, a direct soil-based estimate of deposit age is ambiguous. The stratigraphic position of unit 1 indicates that it is at least middle Pleistocene in age.

3.3 Trench Geologic Structure

As noted in Section 2.0 above, the Sangre de Cristo fault likely consists of at least three fault strands in the site vicinity (Figure 2), including strands associated with: (1) the break-in-slope at the base of the bedrock range front east of the site; (2) a prominent west-facing scarp on the piedmont at the trench site;

and (3) a subtle, broad west-facing scarp on the piedmont about 0.6 km west of the trench site. We believe that the prominent strand traversing our trench site is the primary late Quaternary fault strand, because of its prominent geomorphic expression and continuity across the mountain-front piedmont. Detailed field mapping along the base of the bedrock range front shows that the easternmost strand is not consistently present across late Quaternary deposits. In addition, the western fault strand (west of the trench site, Figure 2) is associated with a very subtle, broad scarp that is much less prominent than the scarp at the trench site. For the purposes of this study, we herein refer to the central strand that traverses the trench site as the primary Sangre de Cristo fault.

Trench T-1 exposed a well-developed eastern fault strand at about Station 26m and a secondary, western fault at about Station 21m (Figures 8, 9, and 10). In the shallow subsurface, the Sangre de Cristo fault is approximately 6 m wide, although it is likely that these two strands merge at a shallow depth below the trench. The eastern fault strand (at about Station 26m) exhibits at least 3 m of late Quaternary vertical displacement, and distinctly different surficial deposits are juxtaposed along this eastern strand. The total amount of vertical displacement across this strand is unknown, and probably is substantially more than 3 m. The fault strand dips about 70˚ east, and juxtaposes middle Pleistocene eolian deposits and alluvium on the east against middle to late Pleistocene alluvium on the west. The eastern fault strand exposed in Trench T-1 clearly displaces the surficial deposits mapped as units 1 through 7 (Figures 8 through 11). Gravel beds within unit 2 are warped into the fault zone and are subparallel to the fault at lower structural levels. Within the fault zone, alluvium is sheared and mixed; unit 7 at Station 26m is mapped as fault gouge developed in the unconsolidated alluvial gravel. The fault zone contains multiple anastomosing strands within the sheared alluvium, with strands commonly bordering lentil-shaped bodies of sediments. On the southern wall of Trench T-1 (Figures 10 and 11), the fault zone includes several vertical or east-dipping fault planes within unit 5, which probably accommodated local strain during down-dropping of the western fault block. The traces of these foliations are at a high angle to the main fault and probably are antithetic Riedel shears. In addition, the fault zone includes multiple vertical strands within units 1 and 2 on the footwall (Figure 10), which decrease in density and degree of shearing progressively to the east. Unit 1 exhibits a far greater number of these sub-vertical shears than unit 2, although this may be related to the massive sandy lithology of unit 1, which may allow for easier perception of shearing than the granular nature of unconsolidated unit 2.

The western fault strand (at about Station 21m) exhibits about 40 cm of vertical displacement of late Quaternary deposits (units 5 and 6, Figures 9 and 10). As noted above, unit 7 along the secondary fault strand is dense, fine-grained, and has little internal shearing. This material probably is fault gouge that has been cemented (“healed”), although locally the margin of unit 7 is faulted (Figure 9). Although the western fault strand does not displace unit 8, the distribution of this unit is spatially associated with the

fault strand. On the southern wall of the trench, unit 8 is a loose, near-vertical tabular body that appears to have filled a fissure. On the northern trench wall, unit 8 filled a triangular-shaped depression, suggesting that the fissure was laterally discontinuous along the fault rupture. As noted above, none of the fault strands exposed in Trench T-1 extends into unit 8 or overlying surficial deposits.

Lastly, the northern trench wall exposed a more complex pattern of deformation on the downthrown block (Figure 9). At about Station 25m, the trench exposed a near-vertical fault with west-down vertical separation, which juxtaposes units 5 and 6. In addition, at about Station 24m, the trench exposed a loose, mixed zone mapped as a series of animal burrows and fissure fills (unit 8). Unit 5 shows a net east-down displacement across this zone, indicating the presence of a 1.5-m-wide graben within the downthrown block adjacent to the eastern fault. Within the graben, unit 5 contains abundant near-vertical stringers of calcium carbonate, which may reflect preferential groundwater percolation along fractures and/or shear planes. On the southern trench wall, there is no evidence of this graben, as the base of unit 5 extends continuously across the exposure. The absence of the graben on the southern trench wall suggests that it is a laterally discontinuous feature and that the trench was located across the southern end of the graben.

4.0 INTERPRETATION AND DISCUSSION

4.1 Paleoseismologic Interpretations

On the basis of stratigraphic characteristics exposed in Trench T-1, units 8, 9 and 10 were deposited locally along the scarp following the most recent surface rupture. Unit 8 was deposited closely following the surface rupture, and filled surface fissures, cracks, and depressions locally along the base of the fresh fault scarp. Unit 9 was deposited soon after the rupture, as the steep, fresh scarp degraded and shed material to the west. This material included coarse gravel clasts derived from the older alluvium (unit 2) uplifted and exposed in the scarp face, and perhaps remnants of units 5 and 6 if they were present on the scarp at the time of the earthquake. Through time, deposition along the scarp produced unit 10, and later unit 11 as the scarp progressively degraded. As noted above, the soil formed on units 9 and 10 is moderately developed, and is suggestive of a latest Pleistocene age, which we speculate to be on the order of about 10,000 to 30,000 years old. Because these units probably were deposited soon after the surface rupture, probably the most recent large earthquake on the southern Sangre de Cristo fault at the Taos Pueblo site probably occurred about 10,000 to 30,000 years ago. Further refinement of this age estimate would require additional studies that are beyond the scope of this preliminary investigation.

On the basis of our detailed topographic profiling (Figure 4), we estimate that the most-recent surface rupture at the site produced approximately 1.5 m of net vertical tectonic displacement (NVTD). This amount seems reasonable taking into account stratigraphic relations exposed in Trench T-1. For example, the maximum thickness of the lower, proximal scarp-derived colluvium (unit ❾, Figure 10) is about 0.8 m, or roughly half of the estimated NVTD. In addition, the total thickness of the scarp-derived colluvium at the primary fault strand also is roughly half of the NVTD estimated from scarp profiling. Because older stratigraphy exposed in the trench is displaced at least 3 m, the trench exposure supports an interpretation of multiple surface ruptures along the Sangre de Cristo fault. Unfortunately, stratigraphic relations in the trench provide no conclusive information on the timing or amount of earlier surface ruptures.

4.2 Hydrogeologic Interpretations

The structural style and deformation features within the fault zone are important characteristics that may influence the flow of shallow groundwater along or across the Sangre de Cristo fault. The fault zone exposed in Trench T-1 is similar to other faults cutting poorly lithified sediments elsewhere in the Rio Grande rift (Rawling et al., 2001). Characteristic features of deformed sediments present in the trench include: (1) rotation of clasts into an orientation subparallel to the fault; (2) foliations in the clay and clayey sand; (3) drag and incorporation of beds into the fault zone; and (4) fault-related mixing of different sediment types. In addition, calcium carbonate cementation commonly exists along fault planes in fine-

and medium-grained deposits, as well as intersecting patterns of subhorizontal and subvertical accumulations that likely are related to vadose-zone groundwater processes.

Based on these observations, it is likely that the hydrologic properties of the fault are grossly similar to others in the rift that have been studied in detail, such as the Sand Hill fault west of Albuquerque (Rawling et al., 2001). Fault drag and mixing of sand and clay creates a heterogeneous fault zone material, and generally reduces pore sizes compared to undeformed materials. In general, in the case of saturated groundwater flow (i.e., below the water table), a fault zone commonly has hydraulic conductivity lower than adjacent sediments, especially gravels and coarse sands (Rawling et al., 2001). However, the saturated hydraulic conductivity of the fault may still be higher than extensively cemented adjacent sediments (such as Unit 6 in our trench). In contrast, in the case of vadose zone groundwater flow (i.e., above the water table) typical in arid and semiarid regions, pore size reductions within the fault zone due to deformation and mixing commonly result in increased unsaturated hydraulic conductivity relative to adjacent gravels and coarse sands (Sigda and Wilson, 2003). Thus, the fault may act as a preferential pathway for unsaturated flow through the vadose zone for downward percolating waters introduced by precipitation and/or surface runoff.

In our trench, unit 6 is pervasively cemented with pedogenic calcium carbonate, and probably has very low permeability, whereas unit 2 is loose alluvium that probably has high permeability. The fault zone exposed in the trench is a mixture of these sediments, and may have a range of permeabilities as a result of tectonic mixing and incorporation of blocks and clasts of the original sediments. We interpret that, in a very general sense, the fault zone probably has a lower permeability than undeformed parts of unit 2, the loose alluvial-fan gravel. In contrast, we interpret that the sheared zones exposed in the trench probably are more permeable than the undeformed parts of the cemented, fine-grained alluvium on the western side of the fault (unit 6; Figure 8). Thus, for downward percolating meteoric waters, and surface runoff that encounters that fault zone, the sheared material probably provides a pathway for downward vadose-zone groundwater flow. In addition, the bulk permeability structure of the fault zone is likely to be anisotropic, such that permeability is lower across the fault than parallel to fault dip, because elongate pods of coarse sediment in the fault may provide high permeability, dip-parallel pathways. The cementation locally observed along the fault exposed in Trench T-1 may be indicative of preferential groundwater flow along the fault.

At the shallow level of exposure in the trench, the displacement on the fault is small, but at deeper levels, where the fault may have experienced multiple rupture events, the fault zone structures are likely to be better developed. In particular, if a continuous, relatively impermeable clay-rich zone is present in the fault zone, the fault at depth can be expected to be a significant barrier to horizontal groundwater flow

below the water table. Based on information gathered from the trench exposure, however, it appears that shallow groundwater flow may preferentially occur downdip along the fault. As shown on Figure 2, the trench site is on a Pleistocene alluvial-fan deposit, above active arroyo drainages that could provide surface water to the fault zone. It is likely that where the fault crosses active arroyos, surface water flows and shallow groundwater encounter shallow levels of the fault zone, which act as relatively permeable conduits for downward groundwater flow.

5.0 CONCLUSIONS

The primary goals of this investigation were to provide information on; (1) large, geologically recent earthquakes along the southern Sangre de Cristo fault on Taos Pueblo lands; and (2) document fault characteristics in the shallow subsurface to help evaluate influences of the fault on vadose zone groundwater flow. The southern Sangre de Cristo fault shows prominent geomorphic evidence of geologically recent surface rupture, including scarps across alluvial fans of various ages, air-photo lineaments, springs, and alignments of vegetation. The Taos Pueblo site was chosen for this investigation because it has: (1) excellent geomorphic relations that constrain the location of the main strand of the fault; (2) late Pleistocene alluvial-fan deposits on the mountain-front piedmont; and (3) minimal cultural disturbance. Detailed topographic surveying of the site vicinity shows that the primary fault scarp across the late Pleistocene alluvial fan exhibits about 3 m of net vertical tectonic displacement. Progressively greater amounts of displacement of older alluvial fan surfaces suggest that the fault has produced multiple surface ruptures within the past several tens of thousands of years or more. In addition, a distinct bevel in the scarp profile at the trench site suggests the occurrence of two surface ruptures since deposition of the alluvial fan, each with about 1.5 m of vertical displacement. These displacements are consistent with large earthquakes having magnitudes in the range of **M**6.5 to **M**7.5.

Stratigraphic relations exposed in the trench across the fault scarp show the presence of middle Pleistocene eolian and alluvial-fan deposits on the western, upthrown side of the fault, and probable late Pleistocene alluvial and colluvial deposits on the eastern, downthrown side of the fault. With the exception of the presently active colluvium, the deposits are not correlative across the fault. Stratigraphic evidence of surface-fault rupture is restricted to a package of scarp-derived colluvium on the downthrown side of the fault. This colluvial package includes fissure-fill and near-scarp deposits that probably were deposited immediately following the surface rupture. We interpret that the moderately developed soil formed on this colluvial package, including soil Btk horizons and stage I calcium carbonate accumulation, is about 10,000 to 30,000 years old. Thus the trench exposure at the Taos Pueblo site suggests that the most-recent surface rupture along the southern Sangre de Cristo fault occurred about 10,000 to 30,000 years ago. Geologic evidence of previous faulting also exists in the form of well-developed fault gouge, more than 3 m of stratigraphic displacement, and fault-scarp morphology, but the timing of this deformation is unconstrained.

The main fault strand at the trench site is located near the base of the topographic scarp, and consists of a primary west-dipping fault plane and secondary faulting within a 6-m-wide zone on the hanging wall. The trench exposure shows the presence of a graben locally at the base of the scarp. The primary fault zone contains multiple anastomosing strands within the sheared alluvium, with strands commonly

bordering lentil-shaped bodies of sediments. The pervasive shearing within the fault zone probably represents a zone of lower permeability compared to surficial deposits east of the fault, but a zone of higher permeability compared to the cemented alluvial deposits west of the fault. The bulk permeability likely is anisotropic with greater permeability down the fault zone rather than across it. Several near-vertical fractures within the fault zone are associated with calcium carbonate accumulations, suggesting that downward percolation of meteoric water occurs preferentially along these fractures. The trench shows the presence of calcium carbonate cementation commonly along fault planes in fine- and medium-grained deposits, as well as intersecting patterns of subhorizontal and subvertical accumulations that likely are related to vadose-zone groundwater processes. The cementation locally observed along the fault exposed in the trench may be indicative of preferential groundwater flow downdip along the fault. Thus, the relations exposed in the trench suggest that major fault strands of the southern Sangre de Cristo fault act as preferential pathways for downward vadose-zone groundwater flow in unconsolidated near-surface materials.

6.0 ACKNOWLEDGEMENTS

This investigation was conducted through collaboration with the New Mexico Bureau of Geology and Mineral Resources, under the supervision of Dr. Paul Bauer. Keith Kelson provided technical oversight, field mapping, and reporting, with assistance throughout the trenching effort from Dr. Dave Love, Sean Connell and Paul Bauer. In particular, Love and Connell described soil-stratigraphic characteristics in the trench and test pits, and fluvial gravel characteristics in the eastern part of the trench. Connell also collected and processed site topographic data with Mark Mansell (NMBGMR, Socorro), who criss-crossed the site for days in the rain and hot sun with differential Global Positioning System equipment. Dr. Geoffrey Rawling (NMBGMR, Socorro) provided interpretations of fault characteristics and structural geologic conditions. Ruben Crespin and Albert Baca (NMBGMR, Socorro) provided invaluable support with trench construction, shoring, and cleaning. Michael Machette (USGS, Denver) graciously visited the trench, logged key parts of the fault trench, and kept the field team under control. William White and Christopher Banet (Bureau of Indian Affairs, Albuquerque) provided technical input on the trench exposure and soil stratigraphy, and augered into the trench floor to provide additional stratigraphic data. This investigation could not have been completed without the efforts and foresight of Nelson Cordova (Taos Pueblo Water Rights), and we are very grateful for his help and support. In addition, we would like to thank Taos Pueblo Warchief Lujan, his staff assistant Louis Zamora, and Tribal backhoe operator John Romero, for help getting the project approved and completed. Lastly, we would like to thank Ms. Evonne Gantz of the New Mexico Department of Public Safety for providing matching funds for this effort and for visiting the site during the investigation.

7.0 REFERENCES

Bauer, P.W., Kelson, K., and Diehl, K., 2001, Geology of the Taos 7.5-minute quadrangle, Taos County, New Mexico: New Mexico Bureau of Geology and Mineral Resources, Open-File Digital Geologic Map OF-DM 44, scale 1:24,000, <http://geoinfo.nmt.edu/statemap/quads/taos/home.html>.

Birkeland, P.W., 1984, Soils and geomorphology: Oxford University Press, 372 p.

Connell, S.D., and Wells, S.G., 1999, Pliocene and Quaternary stratigraphy, soils, and tectonic geomorphology of the northern flank of the Sandia Mountains, New Mexico: implications for the tectonic evolution of the Albuquerque Basin: New Mexico Geological Society, 50th Field Conference, Guidebook, p. 379-391.

Drake, P.G., Harrington, C.D., Wells, S.G., Perry, F.V., and Laughlin, A.W., 1991, Late Cenozoic geomorphic and tectonic evolution of the Rio San Jose and tributary drainages within the Basin and Range/Colorado Plateau transition zone in west-central New Mexico, *in*, Julian, B., and Zidek, J. eds., Field guide to geologic excursions in New Mexico and adjacent areas of Texas and Colorado: New Mexico Bureau of Mines and Mineral Resources Bulletin 137, p. 149-157.

Drakos, P.G., and Reneau, S.L., (unpubl., 2003), Surficial units and processes associated with archaeological sites in selected land conveyance parcels, Los Alamos National Laboratory: Glorieta Geosciences, Inc., Technical Report, 21 p., 5 tables.

Gile, L. H., Hawley, J. W., Grossman, R. B., Monger, H. C., Montoya, C. E., and Mack, G. H., 1995, Supplement to the Desert Project Guidebook, with emphasis on soil micromorphology: New Mexico Bureau of Mines and Mineral Resources, Bulletin 142, 96 p.

Gile, L.H., Hawley, J.W., and Grossman, R.B., 1981, Soils and geomorphology in the Basin and Range area of southern New Mexico-Guidebook to the Desert Project: New Mexico Bureau of Mines and Mineral Resources, Memoir 39, 222 p.

Gile, L.H., Peterson, F.F., and Grossman, R.B., 1966, Morphological and genetic sequences of carbonate accumulation in desert soils: Soil Science, v.101, p. 347-360.

Gonzalez, M.A., 1995, Use of erosional features for tectonics reconstructions and interbasin correlation: an example from the Rio Grande rift, in Bauer, P.W., and 4 others, eds., Geology of the Santa Fe Region: New Mexico Geological Society, 46th Field Conference, Guidebook, p. 139-146.

Grimm, J.P., 1985, The Cenozoic geomorphic history of the Lobo Canyon area of the Mount Taylor volcanic field, Cibola County, New Mexico [M.S. thesis]: Albuquerque, University of New Mexico, 159 p.

Hanks, T.C., and Schwartz, D.P., 1987, Morphologic dating of the pre-1983 fault scarp on the Lost River fault at Doublespring Pass Road, Custer County, Idaho: Bulletin of the Seismological Society of America, v. 77, n. 3, p. 837-846.

Kelson, K. I., and Olig, S.S., 1995, Estimated rates of Quaternary crustal extension in the Rio Grande rift, northern New Mexico: New Mexico Geological Society, 46th Field Conference, Guidebook, p. 9-12.

Kelson, K.I., 1986, Long-term tributary adjustments to base-level lowering northern Rio Grade rift, New Mexico: [M.S. thesis]: Albuquerque, University of New Mexico, 210 p.

Machette, M.N., 1985, Calcic soils of the southwestern United States, *in* Weide, D.L., and Faber, M.L., eds., Soil and Quaternary geology of the southwestern United States: Geological Society of America Special Paper 203, p. 1-42

Machette, M.N., and Personius, S.F., 1984, Quaternary and Pliocene faults in the eastern part of the Aztec quadrangle and the western part of the Raton quadrangle, Northern New Mexico, U.S. Geological Survey Map MF-1465-B, scale 1:250,000.

Machette, M.N., Personius, S.F., Kelson, K. I., Dart, R.L., and Haller, K.M., 1998, Map and data for Quaternary faults in New Mexico: U.S. Geological Survey, Open-file Report 98-521, 443 p.

McDonald, E.V., Reneau, S.L., and Gardner, J.N., 1996, Soil-forming processes on the Pajarito Plateau: investigation of a soil chronosequence in Rendija Canyon: New Mexico Geological Society, 47th Field Conference, Guidebook 47, p. 367-374.

McFadden, L.D., Ritter, J.B., and Wells, S.G., 1989, Use of multiparameter relative-age methods for age estimation and correlation of alluvial fan surfaces on a desert piedmont, eastern Mojave Desert, California: Quaternary Research, v.32, p. 276-290.

Menges, C.M., 1988, The tectonic geomorphology of mountain front landforms in the northern Rio Grande rift, Albuquerque: [Ph.D. dissertation]: Albuquerque, University of New Mexico, 140 p.

Menges, C.M., 1990, Late Cenozoic rift tectonics and mountain-front landforms of the Sangre de Cristo Mountains near Taos, Northern New Mexico: New Mexico Geological Society, 41st Field Conference, Guidebook, p. 113-122.

Munsell Company, 1992, Soil Color Chart: New York, Munsell Company, Kollmorgen Instruments Corporation.

Pazzaglia, F.J., 1989, Tectonic and climatic influences on the evolution of Quaternary depositional landforms along a segmented range-front fault, Sangre de Cristo Mountains, north-central New Mexico [M.S. thesis]: Albuquerque, University of New Mexico, 236 p.

Pazzaglia, F.J., and Wells, S.G., 1990, Quaternary stratigraphy, soils and geomorphology of the northern Rio Grande rift, in Bauer, P.W., Lucas, S.G., Mawer, C.K., and McIntosh, W.C., eds., Tectonic development of the southern Sangre de Cristo Mountains, New Mexico: New Mexico Geological Society, 41st Field Conference, Guidebook, p. 423-430.

Rawling, G.C., Goodwin, L.B., and Wilson, J.L. 2001. Internal architecture, permeability structure, and hydrologic significance of contrasting fault-zone types: Geology v. 29 no. 1, 43-46 p.

Sigda, J.M., and Wilson, J.L., 2003. Are faults preferential flow paths through semiarid and arid vadose zones? Water Resources Research 39(8), doi:10.1029/2002WR001406.

Wong, I.G., Kelson, K. I., and 8 others, 1996, Earthquake potential and ground shaking hazard at the Los Alamos National Laboratory, NM: New Mexico Geological Society, 47th Field Conference, Guidebook, p. 135-142.

Table 1. Description of Pedogenic Soils Exposed in Trenches T-1, T-2, and T-3 at the Taos Pueblo Site.

Trench No. 1. Pedon 1A
10 June 03, Sean D. Connell
Just west of Profile 1B. Buried soils, footwall profile.

Sample	Horizon	Depth (cm)	Color (*moist*)	Texture[1]	Structure	dry sticky	Moist plas	Clay	Gravel (%)	Root	Pore	CaCO3	boundary	Comments
1	Bk1b	0-19	7.5YR 8/2 *7.5YR 5/4*	SCL	2m-csbk	so	vfr	n.o.	1	1f 2vf	1f	e (II)	cs	**Unit 1b:** Top corresponds to channel gravel/mudstone contact in Pedon 1B (top of 3Btb)
2	Bk2b	19-46	7.5YR 8/2 & 6/6 *7.5YR 5/6*	SiCL	2mabk	sh	fr	n.o.	1	1f	1f	ve (II)	cs	carbonate in pore filling only
3	Btk1b	46-66	7.5YR 6/6 & 4/4 *7.5YR 4/4*	SiCL	2m-cabk	sh	fr	2mkpf 1npo	0	1f	2f 1m	e* (I)	gs	1% dark gray Mn stains and 1 cm diameter root casts/Cicadac burrows; carbonate in pore filling only
4	Btk2b	66-87	7.5YR 6/6 & 4/4 *7.5YR 4/6*	SiC	3mpr	h	vfr	1mkpopf	0	1m	2f	e* (I)	cs	**Unit 1a:** 1 cm diameter root casts/cicada burrows; carbonate in pore filling only
5	Btk3b	87-113	7.5YR 6/6 *7.5YR 4/6*	C	2m-cabk 2fpr	h	vfr	1npobr	0	1f	1f-vf	e*	gs	carbonate in pore filling only
6	Bk3b	113-150	7.5YR 6/6 *7.5YR 4/6*	C	3m-cabk	h	vfr	v1npo	0	n.o.	1f-vf	e*	n.o.	carbonate in pore filling only

Table 1. (Continued)

Trench No. 1: Pedon 1B
10 June 03, Sean D. Connell: footwall profile.

Sample	Horizon	Depth (cm)	Color (*moist*)	Texture	Structure	dry sticky	Moist plas	Clay	Gravel (%)	Root	Pore	CaCO3	boundary	Comments
13	C	0-3	7.5YR 4/4 *7.5YR 3/4*	SL	sg	lo ss	lo ps	n.o.	<1	n.o.	n.o.	eo	As	**Unit 11:** slightly hydrophobic; contains minor dark gray organic matter
12	Btk1	3-14	7.5YR 4/4 *7.5YR 3/3*	SCL	2m-c sbk	so	lo	1nco	<2	2f-vf	1vf	es (dissem)	cs	
11	Btk2	14-26	7.5YR 4/3 *7.5YR 3/3*	SCL	2m sbk	so	so	1nbr	<2	1f	1f	es (l)	cs	
10	Bk3	26-43	7.5YR 5/2 *7.5YR 4/4*	LS	1m sbk	sh	fi	v1nco	<5	1f 2co	1f-m	es (l)	cs	
9	2Bk1b	43-59	7.5YR 8/1 *7.5-10YR 7/3*	LS	1m abk	sh ss	fr po	n.o.	10	1f	1f-m	ev (III)	cs	**Unit 2:**
8	2Bk2b	59-101	7.5YR 8/1-2 *7.5YR 5/3*	SL	sg-1m sbk	lo so	lo po	n.o.	30-40	2f-vf	n.o.	ev (II+)	cw	local uncemented gravel with primary bedding fabric preserved
7	2Bk3b	101-113	7.5YR 8/1 *7.5YR 8/2-7/4*	SL	sg	lo so	lo po	n.o.	10	3vf	n.o.	ev (II+)	as	loose
6	2Bkmb (K)	113-117	7.5YR 7/4 *7.5YR 5/4*	LS	m	h sh	vfi po	n.o.	5	1vf	1vf 2co	ev (n.a.)	as	gully bed (groundwater) cementation(?)
5	2Bk1b	117-162	7.5YR 8/1 *7.5YR 8/2-7/4*	LS	sg	lo so	lo po	v1nco	40	1vf	n.o.	ve (l)	as	carbonate on clast undersides; matrix contains no carbonate
4	2Btk2b	162-226	7.5YR 5/4 *7.5YR 4/3*	LS	sg	lo so	lo po	1mkpf 1nco	60	1f	n.o.	es (I+)	aw	carbonate on clast undersides; matrix contains no carbonate
3	3Btb	226-246	7.5YR 4/6 *7.5YR 4/4*	C	2fpr 1m-cabk	sh s	fr mp-p	3mkpfpo	0	n.o.	2f	eo	cs	**Unit1:** manganese stains on ped faces
2	3Bb1	246-267	7.5YR 5/6 *7.5YR 4/6*	C	2m-cabk	sh s	vfr mp-p	n.o.	0	n.o.	2co 1f	eo	cs	1-2% Mn stains on ped faces
1	3Bb2	267-279	7.5YR 5/6-4 *7.5YR 4/4*	C	2mabk	sh s	vfr mp-p	v1npo	0	n.o.	1vf	eo	n.o.	1-2% Mn stains on ped faces

Two distinct ages of krotovina based on cementation. Older white, moderately cemented krotovina, and younger, brown, loose, weakly cemented krotovina.

Table 1. (Continued)

Trench No. 1. Pedon 1C: hangingwall profile
11 June 03, Sean D. Connell

Sample	Horizon	Depth (cm)	Color (*moist*)	Texture	Structure	dry sticky	Moist plas	Clay	Gravel (%)	Root	Pore	CaCO3	boundary	Comments
1	B	0-11	7.5YR 4/4 *7.5YR 3/3*	SiCL	2-3c abk	sh ss	vfr ps	vlnco	1-2	1vf-f	1f	eo	cs	**Unit 11:**
2	Btk1	11-29	7.5YR 5/4 *7.5YR 4/3-4*	SiCL	2-3m-c sbk	sh s	vfr ps-mp	vlnpo 1ncopf	<2	1f-m	1f	ve-e	cs	7.5YR 4/3 clay on ped faces
3	Btk2	29-44	7.5YR 5/4 *7.5YR 5/4*	C	2m-c abk 3fpr	sh s	vfr mp	1npopf	<2	1f-m	2vf-f	e (I)	cs	**Unit 10:** 7.5YR 8/2 carbonate in pores and ped faces; sparse 2-mm diameter soft carbonate nodules
4	Btk3	44-66	7.5YR 6/4 *7.5YR 5/4*	C	3fpr 2m abk	h s	fr mp	1npf	<2	1f-m	2vf-f	es (I+)	gs	7.5 YR 7/1 carbonate in pores and few ped faces
5	Btk4	66-101	7.5YR 6/6 *7.5YR 5/6*	C	3fpr 2m-c abk	h s	fr mp	1nbrpf	<2	1f	1vf-f	e (I+)	cw	7.5 YR 8/1 carbonate in pores and many ped faces
6	Btkb	101-125	7.5YR 6/6 *7.5YR 5/6*	C	2m-c abk	sh s	vfr mp	2mkbrpf	<5	n.o.	1vf	ve (I+)	aw	**Unit 9:** carbonate in pores
7	2Bkmb1	125-145	7.5YR 8/4 *7.5YR 7/4*	C	1f-m abk	h ss	vfr mp	n.o.	<2	1f	2vf-f	ev (III)	cw	**Unit 6:**
8	2Bkmb2	145-197	10YR 7/3 *7.5YR 7/4*	C	1f abk	sh ss	vfr mp	n.o.	<2	1vf	2f	ev (III)	gi	1npf clay obscured by carbonate
9	2Bkmb3	197-215	10YR 7/3 *10YR 6/6*	C	1f-m abk	so ss	vfr mp	n.o.	<5	n.o.	1vf	ev (III)	cw	**Unit 5:** 20-30%, 5-20 cm kroatovina (7.5 YR 5/3d, 4/4m); carbonate cements decrease downward from ev –eo
10	2Bkmb4	215-233	10YR 8/3 *10YR 7/3*	SCL	1f-m abk sbk	h ss	vfr ps	1npf	<5	n.o.	n.o.	ev (III)	ci	**Unit 4:**
11	3Bkb	233-248	7.5YR 6-5/4 *7.5YR 4/3*	SCL	sg-1f sbk	sh ss	vfr ps	v1copf	20	n.o.	n.o.	e	n.o.	**Unit 3:**

Table 1. (Continued)

Trench No. 2
09 June 03 Sean D. Connell

Sample	Horizon	Depth (cm)	Color (*moist*)	Texture	Structure	dry sticky	Moist plas	Clay	Gravel (%)	Root	Pore	CaCO3	boundary	Comments
1	C	0-5	7.5YR 5/4 *7.5YR 4/3*	SC	sg	lo	lo	n.o.	<2	3vf	n.o.	eo	as	
2	Bt1	5-22	7.5YR 4/4 *7.5YR 3/3*	SiC	3m-cabk	h ss	vfr mp	1mkbrpf	0	2mco	2fvf	eo	gs	
3	Bt2	22-35	7.5YR 4/4 *7.5YR 3/3*	C	2mpr	h ss	vfr mp-p	1mkpfpo	0	2co 1m	1vf 2f	eo	cs	
4	Btk3	35-63	7.5YR 5/4 *7.5YR 4/4*	C	2mabk	h ss	fr mp-p	1npf	<2	2f	1f	es (I)	cs	
5	Btk4	63-77	7.5YR 5/6 *7.5YR 4/6*	C	3fpr 2mabk	h s	fr mp-p	1npo	3	n.o.	2f-m	es (II)	cw	scattered gravel; 7.5YR 8/2 carbonate mottles (c1p)
6	Btk5	77-94	7.5YR 5/6 *7.5YR 4/6*	C	3mabk 2fpr	h s	fr p	1npopf	<2	n.o.	2f	es (II)	cs	
7	Btk6	94-110	7.5YR 5/6 *7.5YR 4/6*	C	2fpr	h s	fr p	1n-mkpfco	<2	n.o.	2f	es (II+)	ci-ai	top defined by stone line
8	2Bkmb	110-162	N8/0-7.5YR 8/2 *7.5YR 6/6*	CL	1fpl 2m-cabk	sh ss	vfr ps	n.o.	3	2f	2fvf	es (III+)	cw	upper 20-30 cm contains discontinuous 2mpl structure on west wall
9	2Bkb1	162-247	7.5YR 7/3 *7.5YR 5/4*	CL-SCL	2m-csbk	so ss	vfr ps	n.o.	<2	n.o.	1f	ev (II+)	cw	
10	2Bb	247-267	7.5YR 5/6 *7.5YR 4/6*	CL	2vf-fabk	so ss	vfr ps	v1ncopo	0	n.o.	2f	eo (I+)	cw	discontinuous
11	2Btb2	267-300	7.5YR 4/6 *7.5YR 4/6*	C	2fpr	sh s	vfr p	2mk-kpf	10-20	1f	2f	ve (I+)	n.o.	carbonate only in pore linings

Table 1. (Continued)

Trench No. 3
09 June 03, Sean D. Connell

Sample	Horizon	Depth (cm)	Color (*moist*)	Texture	Structure	dry sticky	Moist plas	Clay	Gravel (%)	Root	Pore	CaCO3	boundary	Comments
	Disturbed	0-2	n.d.	n.d.	n.d.	n.d.	n.d.	n.d.	n.d.	n.d.	n.d.	n.d.	n.d.	not described (n.d.)
1	C	2-5	7.5YR 4/3 *10YR 4/3*	SiC-C	sg	lo ss	lo mp	n.o.	7	2vf 1f	n.o.	eo	as	scattered clasts due to bioturbation; **wind-blown clay**
2	AB	5-10	7.5YR 4/4 *7.5YR 3/3*	SiC	sg	lo s	lo p	n.o.	5	3vf 1f	n.o.	eo	as	
3	Bt	10-14	7.5YR 5/4 *10YR 4/3*	SiC-C	sg-1msbk	so s	lo p	1nbr	5	2f	n.o.	eo	as	7.5YR 6/6 fine-grained sand coatings on ped faces
4	Btkb1	12-30	7.5YR 4/4 *7.5YR 4/4*	C	1msbk	sh s	vfr p	2mk-kpfpo	35	2fm	2f	ve (I)	as	**Young alluvium:** thin calcium carbonate coatings on clast undersides; local thin gravel channels
5	Btkb2	30-50	7.5YR 5/4 *7.5YR 4/4*	SC	3f-mabk	h s	vfr p	2mk-kpfpo	10	2co 2m	2fvf	es-ev (I+)	cw	7.5YR 6/4 carbonate mottles (c23d)
6	2Bkmb1	50-68	10YR 8/2-3 *7.5YR 7/4*	SCL	2m-cabk	h ss	vfr mp	v1nco	5	2m	n.o.	ev (III+)	gs	**Older alluvium**: upper ~10-20 cm contains mottles and infills of overlying material; Q: erosional ctc???
7	2Bkmb2	68-96	10YR 8/1-2 *7.5YR 7-6/4*	SL(?)	3c-vcpl	h ss	vfr mp	1nbrpo	10	1f	1f	ev (III+)	cs	
8	2Bkmb3	96-124	10YR 8/3 *10YR 6/4*	SCL	2vcpl	h ss	vfr mp	n.o.	30	n.o.	2vf	ev (III+)	gs	carbonate mottles (m3d)
9	2Bkb1	124-151	10YR 8/2 *7.5YR 5/4*	SCL	2cabk	h s	vfr mp	v1nbr	5-15	1m	1fm	ev (II+)	gs	carbonate mottles (m3d)
10	2Bkb2	151-169	10YR 6/4 *10YR 4/4*	SCL	m	lo ss	lo ps	n.o.	<5	n.o.	n.o.	ev	n.o.	

Profile is 0.3 m east of northwest access trench/main trench intersection.

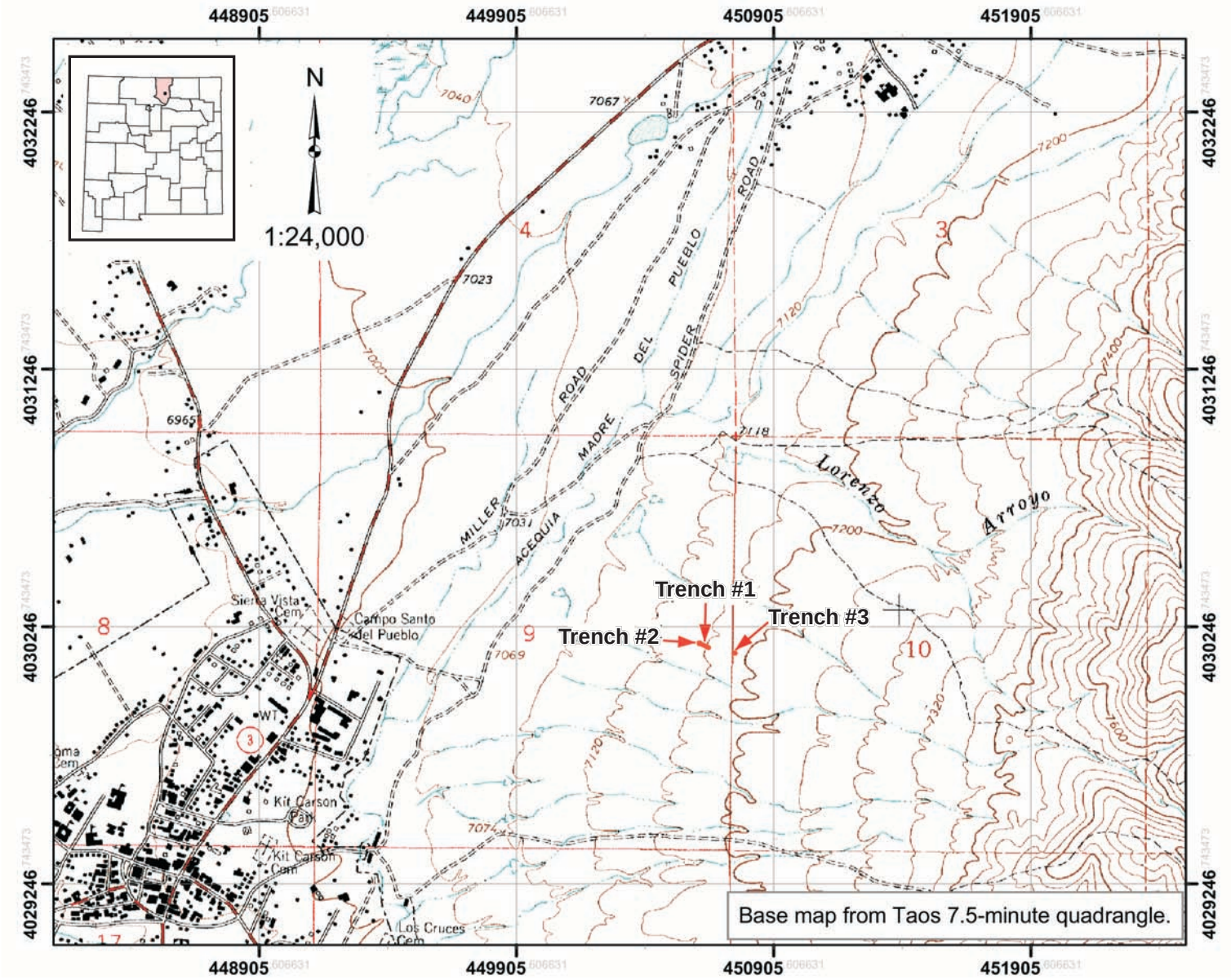

Figure 1. Index map showing location of trenches at the Taos Pueblo trench site.

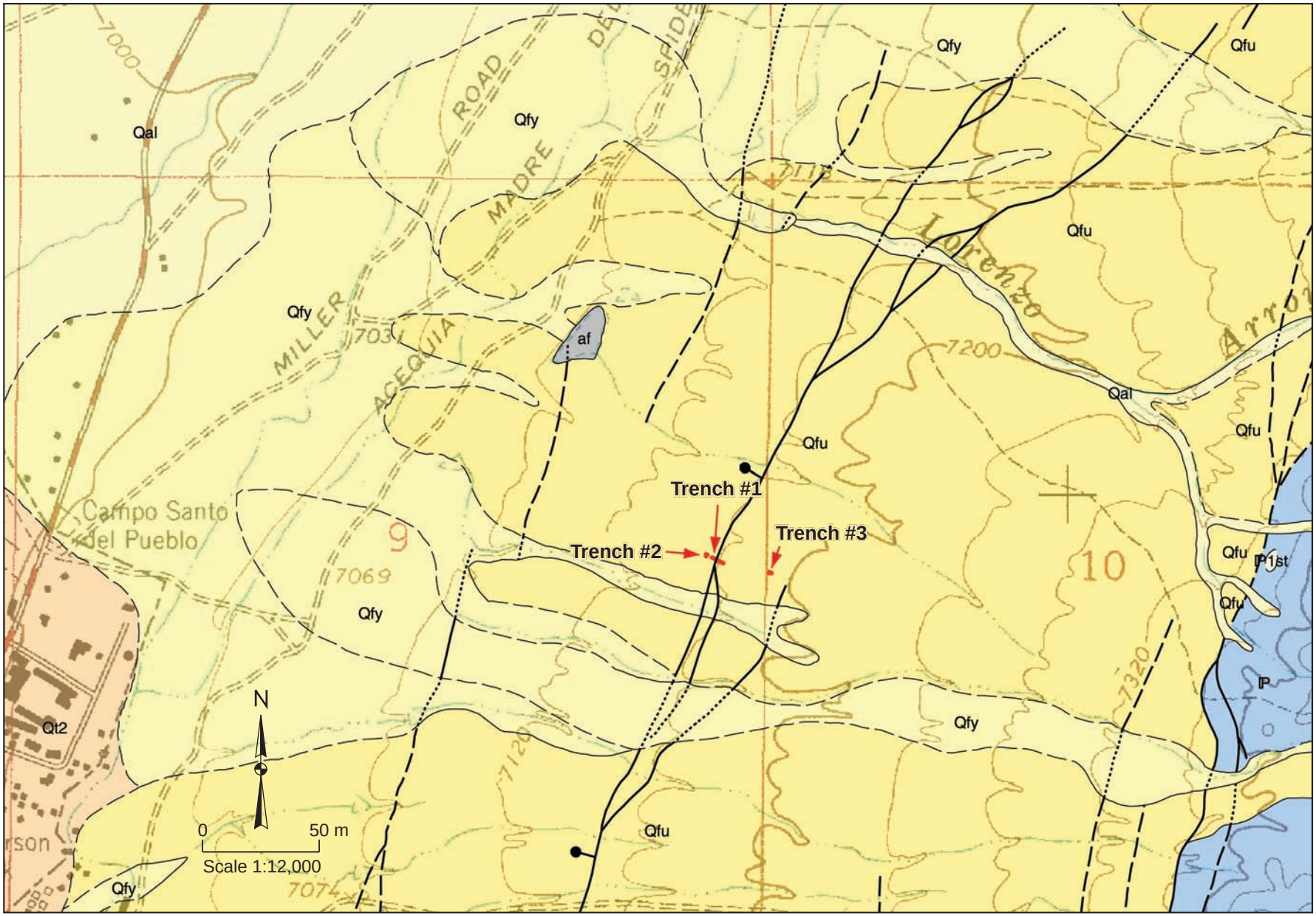

Geology from Bauer and Kelson

Figure 2. Geology map of the area surrounding the Taos Pueblo trench site.

Figure 3. Photograph looking east toward Trench T-1, showing differential GPS survey equipment (being used by Sean Connell and Mark Mansell), and electronic survey equipment used for documenting the trench exposure.

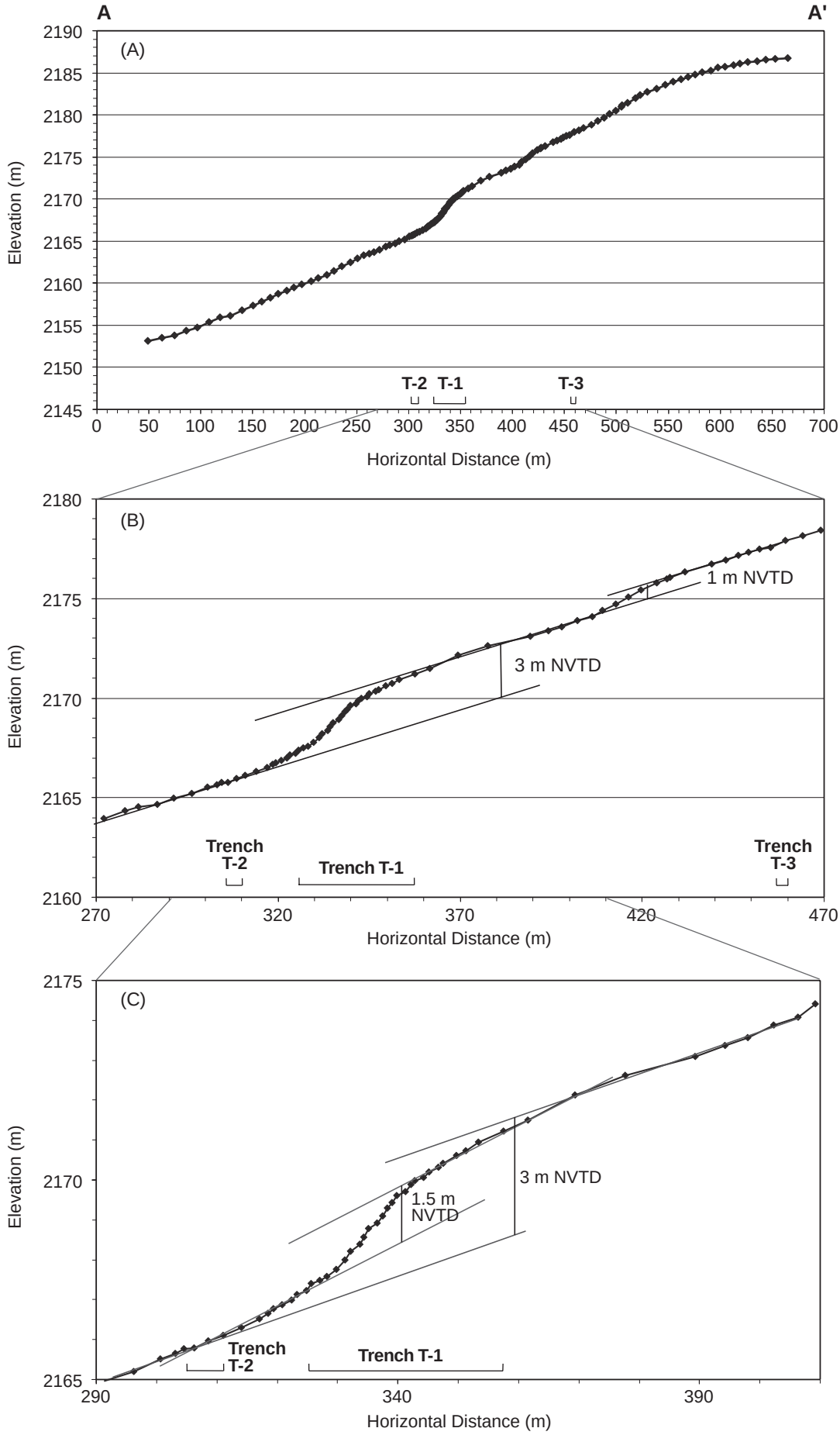

Figure 4. Topographic profiles across the Sangre de Cristo fault zone of the Taos Pueblo trench site, showing estimated net vertical tectonic displacement.

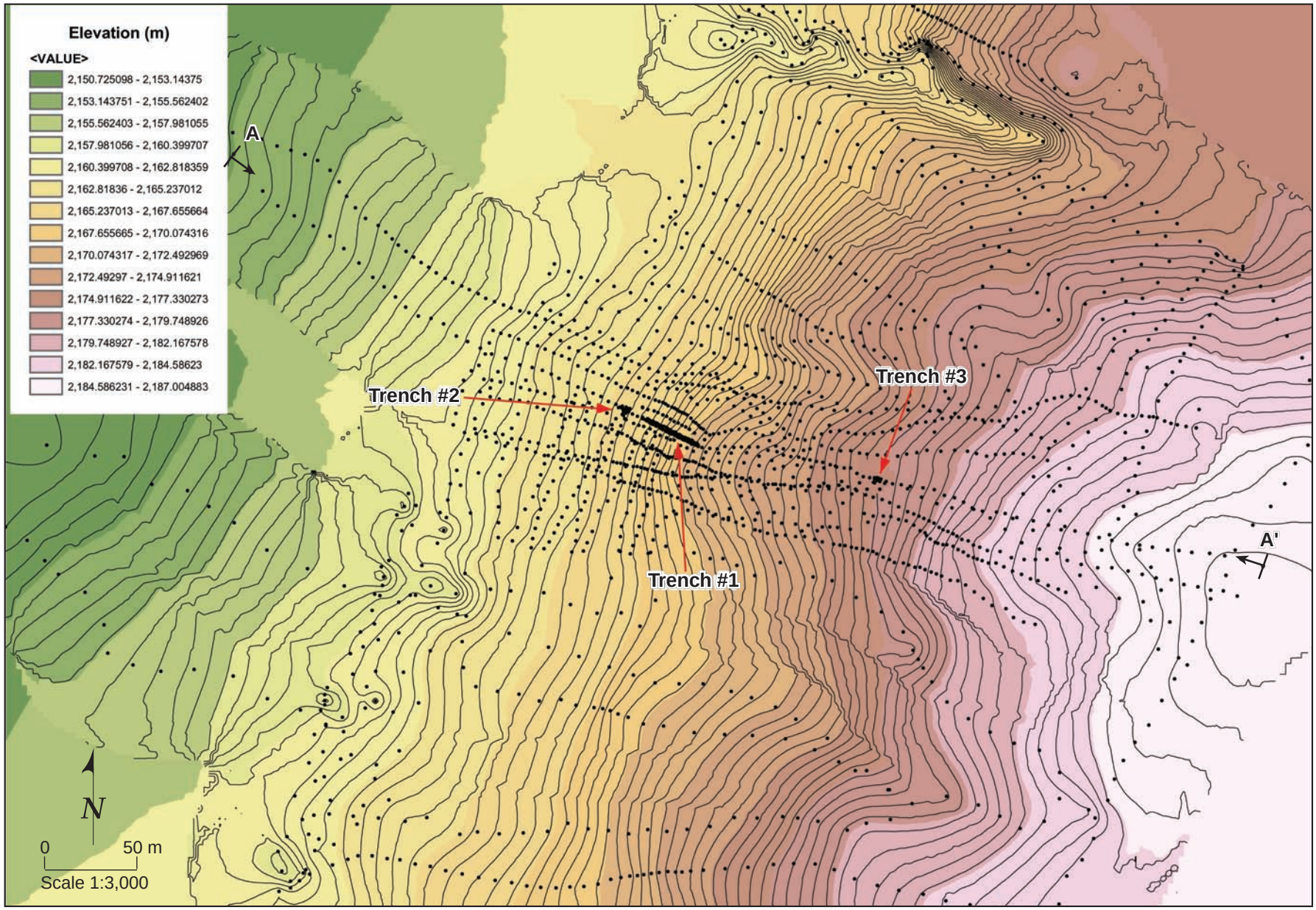

n = 1794 GPS points

Figure 5. Detailed topographic map of the Taos Pueblo trench site, derived from differential GPS survey in June, 2003.

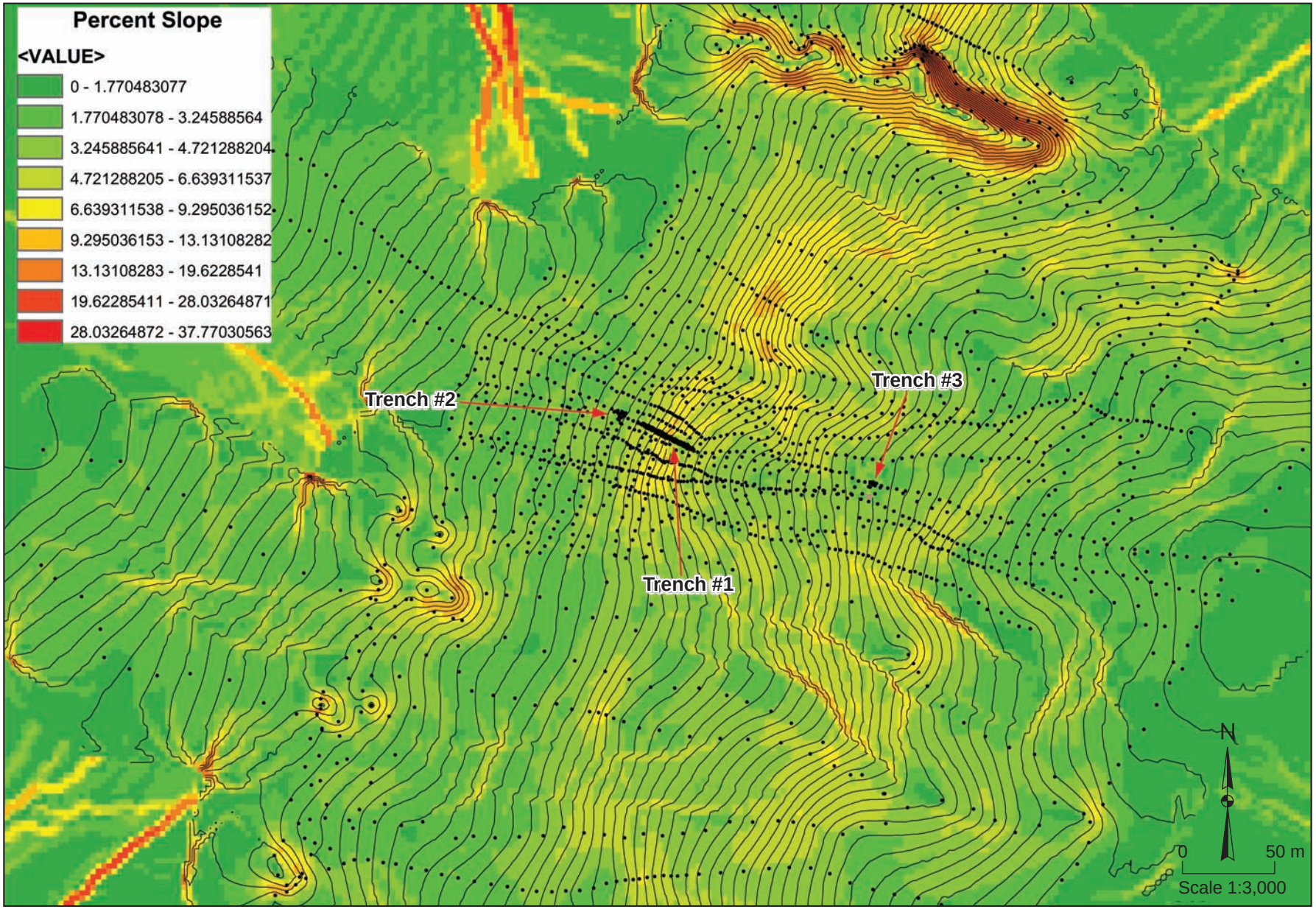

n = 1794 GPS points

Figure 6. Slope map derived from detailed topographic surveying at the Taos Pueblo trench site.

Figure 7. Photographs of the Taos Pueblo Trench site, looking east.

TAOS • SANGRE DE CRISTO FAULT

Log of Trenches 1 and 2

TRENCH 2
NORTH WALL

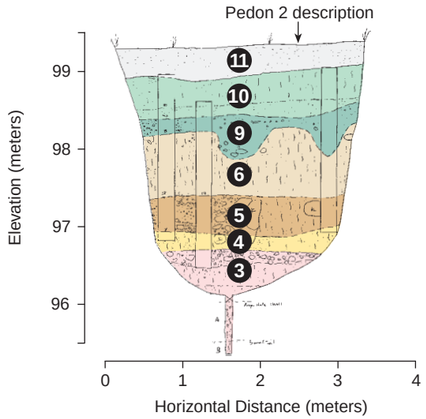

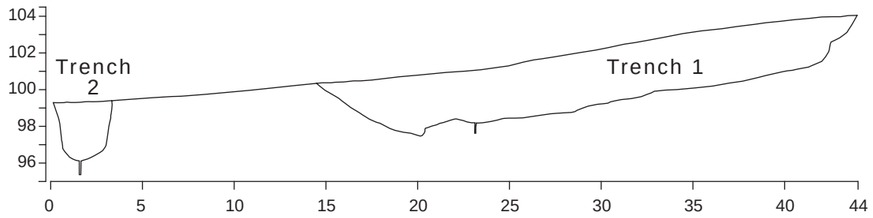

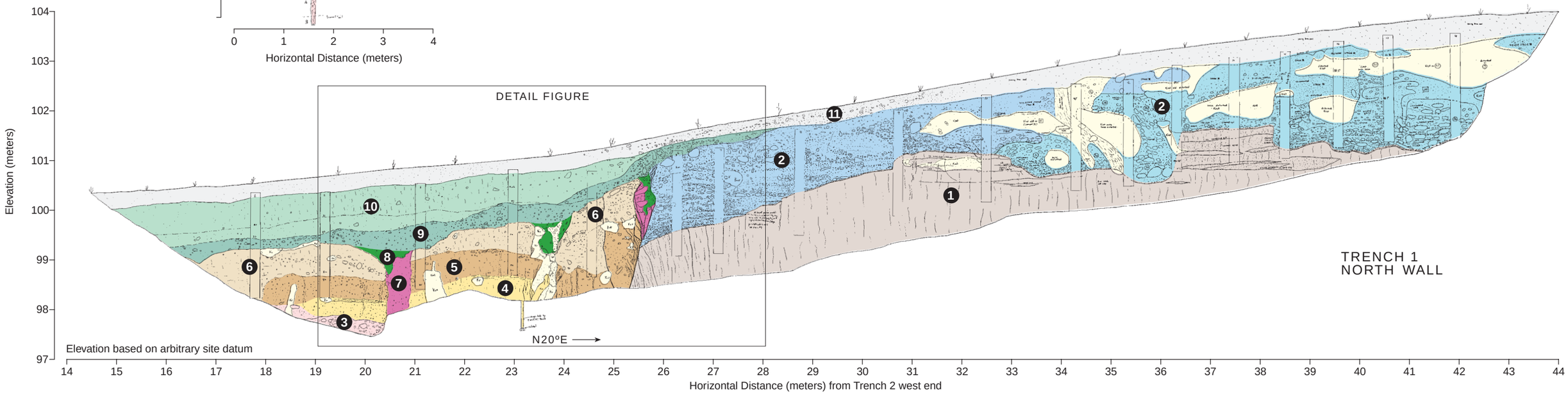

TRENCH 1
NORTH WALL

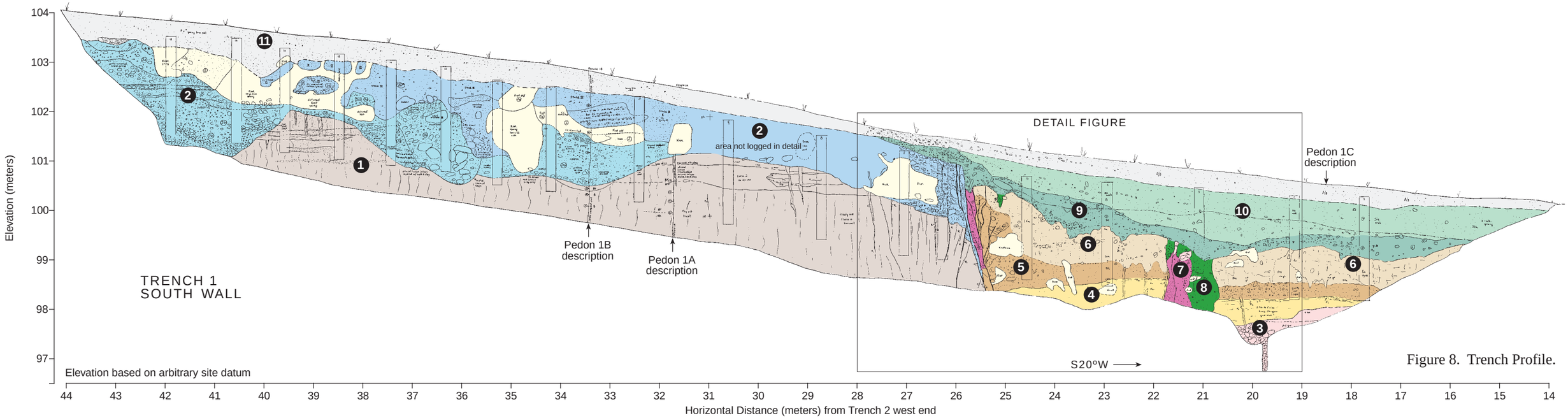

Figure 8. Trench Profile.

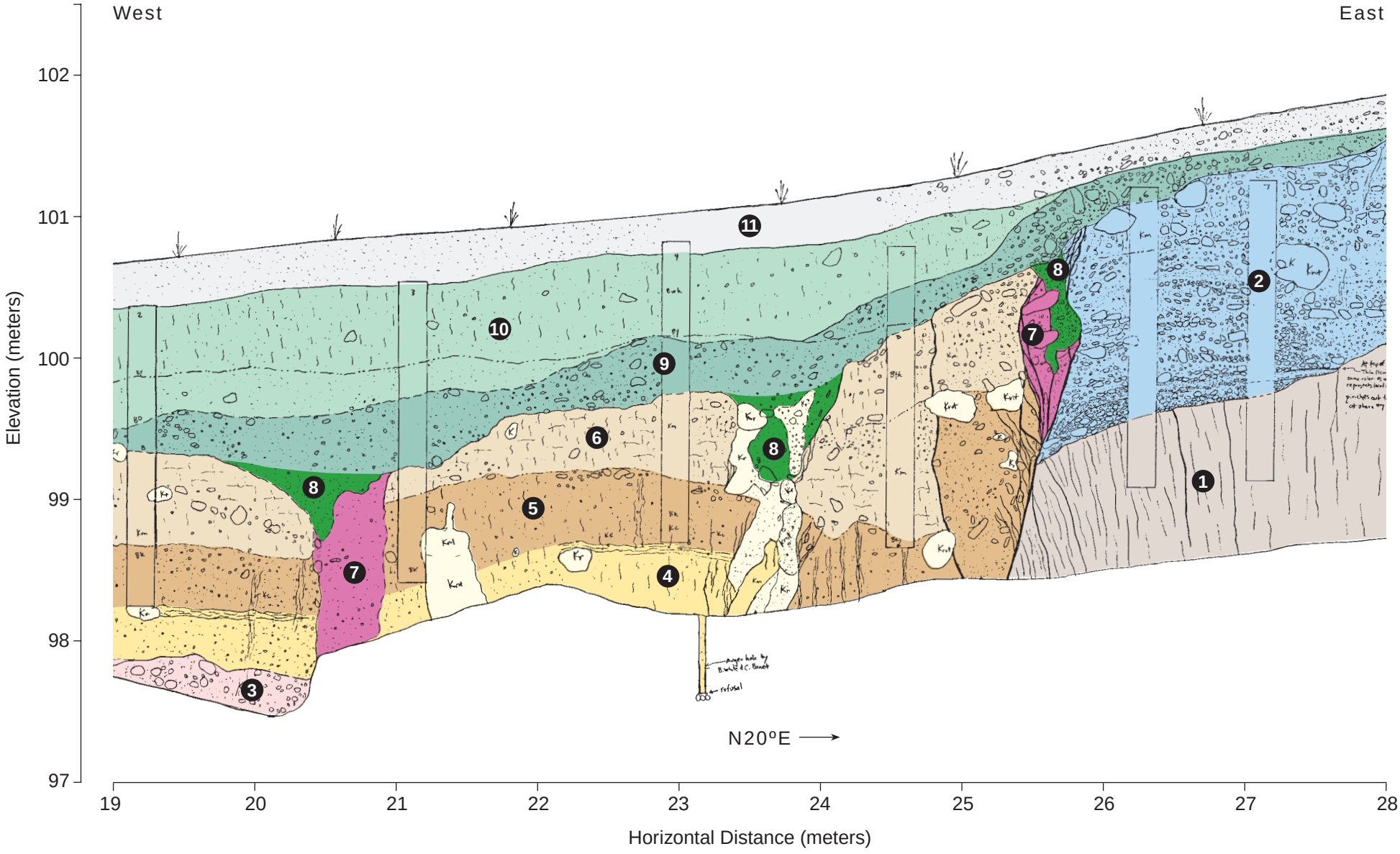

Figure 9. North wall

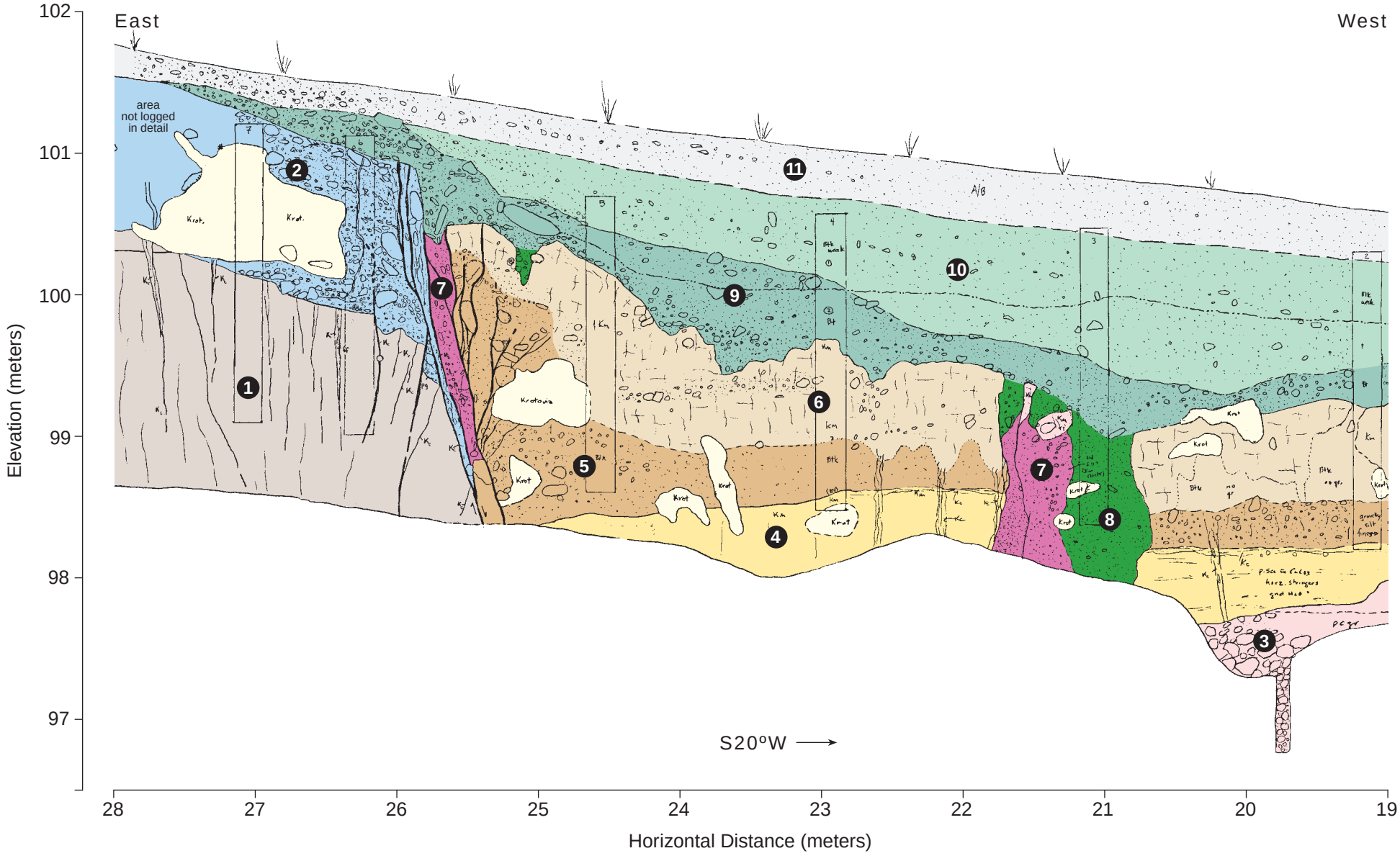

Elevation based on arbitrary site datum

TAOS • SANGRE DE CRISTO FAULT

Detailed Log of Trench 1
(South Wall, Central Portion)

Figure 10. South wall.

LITHOLOGIC DESCRIPTION

(see appendix for additional pedogenic descriptions)

Unit 11: Late Holocene colluvium; (7.5YR4/4) SILTY SAND to CLAYEY SAND. Fine to coarse sand; subrounded to subangular gravel up to 5 cm; 20 to 30% gravel between stations 26 and 29 m; less than 5% gravel west of station 215 m grading to no gravel west of station 21 m; poorly sorted; dry, slightly hard to loose; bioturbated; footwall exposures contain clasts of underlying pedogenic Stage III soil of unit 2; upper 10 to 20 cm contains no pedogenic calcium carbonate; lower part ranges to Stage 1; locally overlies hearth and deposit containing black smudge-ware potsherd; (ACTIVE HILLSLOPE COLLUVIUM).

Unit 10: Late Pleistocene colluvium. Brown to light brown (7.5YR 5/4 to 7.5YR 6/4) SANDY CLAY. Fine to coarse sand; subrounded to subangular gravel up to 10 cm; up to 5% gravel, with more gravel closer to fault and in upper parts of unit; locally contains discontinuous, gently west-dipping gravel stone lines; poorly sorted; dry, slightly hard to hard; contains up to stage I+ calcium carbonate (soil Btk horizons); calcium carbonate nodules; slightly effervescent; gradual smooth basal contact; (TECTONIC SCARP-DERIVED DISTAL COLLUVIUM).

Unit 9: Late Pleistocene colluvium. Reddish yellow (7.5YR 6/6) SANDY CLAY to SANDY GRAVEL. Fine to coarse sand; subrounded to subangular gravel up to 40 cm; 20 to 30% gravel in eastern part of unit (near stations 24 to 28 m); 5 to 15% gravel in western part of unit (west of station 24); slightly smaller gravel clasts progressively westward; smaller gravel clasts progressively upward, especially near stations 23 to 26 m (adjacent to primary fault); clast rounding, size, lithology, and location suggests derivation from unit 2 on hanging wall; locally contains discontinuous, gently west-dipping gravel stone lines; poorly sorted; dry, hard; contains up to stage I+ calcium carbonate (soil Btk horizon); slightly effervescent; unit is not faulted by primary or secondary faults in underlying deposits; grades upward into unit 10; clear smooth basal contact; (TECTONIC SCARP-DERIVED PROXIMAL COLLUVIUM).

Unit 8: Late Pleistocene (?) fissure fill / fault gouge. Reddish yellow (7.5YR 6/6) SAND WITH GRAVEL. Fine to coarse sand; subrounded to subangular gravel up to 10 cm ; 10 to 20% gravel; map unit consists of several separate, triangular-shaped bodies along the primary fault near station 25 and associated with secondary faults near stations 21 and 24 m (northern wall only); contain gravel clasts having vertical orientations that are sandstone clasts similar to those in unit 2 and CaCO3-rich sand similar to that of unit 6; all subunits appear to be basal parts of overlying unit 9; poorly sorted; dry, hard; clear irregular lateral margins.

Unit 7: Late Pleistocene (?) fault gouge. Reddish yellow (7.5YR 6/6) SAND WITH GRAVEL. Fine to coarse sand; subrounded to subangular gravel up to 30 cm but commonly less than 10 cm; 10 to 20% gravel; map unit consists of two separate, near-vertical bodies, one along primary fault near station 25 m and one associated with secondary fault near station 21 m; both contain gravel clasts having vertical orientations; eastern sub-unit (within primary fault zone) is pervasively sheared and contains sandstone clasts similar to those in unit 2; western sub-unit (near secondary fault zone) does not appear to be sheared, and contains only subangular clasts of CaCO3-rich sand similar to unit 6; poorly sorted; dry, hard; clear smooth lateral margins.

Unit 6: Middle to Late Pleistocene (?) alluvium. Pink (7.5YR 8/4) CLAYEY SAND. Fine to coarse sand; subrounded to subangular gravel up to 15 cm; 5% gravel, locally within discontinuous beds that dip gently eastward toward the primary fault (on southern wall near station 24 m) or toward the secondary fault (on northern wall near station 20 m); poorly sorted; dry, hard; contains stage III calcium carbonate (soil Bkm horizon); pervasive calcium carbonate throughout deposit; strongly effervescent; unit is sheared and faulted adjacent to faults near stations 21 and 24 m; gradual irregular basal contact.

Unit 5: Middle to Late Pleistocene (?) alluvium. Very pale brown (10YR 7/3) SAND WITH GRAVEL. Fine to coarse sand; subrounded to subangular gravel up to 20 cm, with larger clasts adjacent to primary fault near station 25 m and adjacent to secondary fault near station 21 m; 10% gravel directly west of primary fault zone near station 25 m and directly west of secondary fault zone near station 21 m; lower percentage (<5%) of gravel elsewhere; massive; poorly sorted; dry, hard; contains stage III calcium carbonate (soil Bkm horizon); effervescent; unit is sheared and faulted adjacent to faults near stations 21 and 25 m; clear smooth basal contact.

Unit 4: Middle to Late Pleistocene (?) alluvium. Very pale brown (10YR 7/3) SILTY SAND. Fine to coarse sand; subrounded to subangular gravel up to 5 cm; <5% gravel; massive; dry, hard; contains subhorizontal and subvertical stringers of calcium carbonate (likely related to groundwater precipitation); effervescent; clear wavy basal contact.

Unit 3: Middle to Late Pleistocene (?) alluvium. Light brown to brown (7.5YR 5/4 to 7.5YR 6/4) SANDY GRAVEL, grading upward to very pale brown (10YR 7/3) GRAVELLY SAND. Fine to coarse sand; subrounded to subangular gravel up to 30 cm in lower part; effervescent; massive; dry, hard; basal contact not observed.

Unit 2: Middle Pleistocene (?) alluvium. Strong brown (7.5 YR 6/4 to 7.5YR 6/6) pebble to boulder GRAVEL; 40 to 60% subrounded to subangular gravel clasts up to 36 cm; locally map unit contains finer gravel sub-units with clasts less than 10 cm, and very coarse gravel sub-units with clasts ranging from 10 to 36 cm; lower exposures loose; upper part pedogenically modified and cemented pebbly sandstone and conglomerate; strongly effervescent; extensively bioturbated; stage III pedogenic calcium carbonate horizon. Lower part includes irregular bodies of gravel, loose to well cemented with calcium carbonate; carbonate appears concentrated in subvertical pipe-like structures and in subhorizontal bedding; locally cemented by white (N 8/0) 1 to 2 mm thick calcium carbonate rinds. Clast and matrix-supported gravel exhibits horizontal- to low-angle cross-stratified beds to 2 m thick; well bedded; thinly bedded to laminated in sets 3-5 cm thick; abrupt smooth basal contact.

Unit 1: Middle Pleistocene (?) intermixed alluvium and loess. Strong brown (7.5YR 4/6 to 7.5YR 5/6) SAND, SILT, and CLAY (divided into upper (1b) and lower (1a) sub-units). Sub-unit 1b: Pinkish white (7.5YR 8/2 to reddish yellow (7.5YR 6/6) SANDY SILT with CLAY; slightly hard; moderately effervescent to non-effervescent; subvertical carbonate-filled fractures taper from 4 cm to fine cracks up to 55 cm long are exposed between stations 33 and 32 m and between stations 39 and 40 m; clear smooth basal contact. Sub-unit 1a: Reddish yellow (7.5YR 6/6) to strong brown (7.5YR 4/6) CLAYEY SILT; dense, weakly to non-effervescent; locally contains 1 cm diameter cicada burrow casts; locally contains 3 to 30 cm thick silty sand beds with low-angle cross beds; poorly sorted; 10-15% of lower unit locally; basal contact not exposed.

Figure 11. Photograph of the northern wall of Trench T-1, at the exposure of the main fault (stations 26 and 25 m). Red flagging denotes faults; pink flagging denotes fractures; all other colors denote stratigraphic contacts.